Single-Molecule Electronics: Chemical and Analytical Perspectives

Richard J. Nichols and Simon J. Higgins

Department of Chemistry, University of Liverpool, Liverpool L69 7ZD, United Kingdom; email: R.J.Nichols@liverpool.ac.uk

Annu. Rev. Anal. Chem. 2015. 8:389–417

First published online as a Review in Advance on June 1, 2015

The *Annual Review of Analytical Chemistry* is online at anchem.annualreviews.org

This article's doi: 10.1146/annurev-anchem-071114-040118

Keywords

single-molecule conductance, scanning tunneling microscope, molecular electronics, single molecules, mechanically controlled break junction, organic electronics, molecular wires

Abstract

It is now possible to measure the electrical properties of single molecules using a variety of techniques including scanning probe microcopies and mechanically controlled break junctions. Such measurements can be made across a wide range of environments including ambient conditions, organic liquids, ionic liquids, aqueous solutions, electrolytes, and ultra high vacuum. This has given new insights into charge transport across molecule electrical junctions, and these experimental methods have been complemented with increasingly sophisticated theory. This article reviews progress in single-molecule electronics from a chemical perspective and discusses topics such as the molecule-surface coupling in electrical junctions, chemical control, and supramolecular interactions in junctions and gating charge transport. The article concludes with an outlook regarding chemical analysis based on single-molecule conductance.

1. INTRODUCTION

The genesis of the field of molecular electronics is considered by many to be Aviram & Ratner's (1) theoretical suggestion in the early 1970s to create a diode from molecular donor and acceptor sites separated by a nonconjugated σ-bonded tunneling bridge. At that time, it was not possible to make defined electrical measurements even on molecular monolayers; however, it was indeed shown later that Langmuir-Blodgett films of potential organic molecular rectifiers could be formed and sandwiched between electrode contacts, demonstrating diode behavior (2). More recently, reliable electrical measurements on even single molecules were made possible. The amazing feat of tethering single molecules between pairs of electrodes and electrically interrogating them is the result of the development of several techniques such as the mechanically controllable break junctions (MCBJs), scanning probe microscopies, and precision lithographic fabrication of nanoelectrode gaps. This ability to measure the electrical properties of single molecules has given molecular electronics a defined new identity compared to the more mature field of organic electronics. Generally in organic electronics, bulk properties of organic materials, commonly polymers, are utilized, distinguishing organic electronics from the nascent field of single-molecule electronics. Single-molecule devices are at a much earlier stage of evolution than organic electronic devices, which have been successfully rolled out in technologies such as organic polymer light-emitting displays. Although commercial implementation of single-molecule devices may appear to be a distant dream, single-molecule electrical measurements and associated theory are greatly contributing to the fascinating issue of how charge can be transported across molecules. This has relevance to other fields such as electrochemistry, biophysics, nanotechnology, and molecular photovoltaics.

The single-molecule electrical methods now go beyond measurement of solely junction conductance, with measurements of, for instance, the temperature dependence of single-molecule conductance, single-molecule thermoelectric properties, simultaneous molecular conductance and junction stretching force, electrochemical gating, and transition voltage. Such studies make it possible to perform detailed mechanistic studies of charge transport across single molecules, and these have given many new details that were not apparent from measurements on large area junctions. There are several reviews of single-molecule electronics; see References 3–10 for examples. We focus on chemical aspects of single-molecule junctions, for example chemical anchoring groups and binding to the electrodes, supramolecular interactions, and electrochemical switching in single-molecule electrical junctions. In Section 8, we offer a perspective on chemical detection of species in single-molecule electrode gaps and anticipate that analysis may be one of the first technological implementation areas for single-molecule electronics.

2. TECHNIQUE FOR MEASURING SINGLE-MOLECULE ELECTRICAL PROPERTIES

Before discussing chemical aspects of single-molecule electrical junctions, we provide a brief overview of the key techniques for measuring single-molecule electrical properties. There are several techniques that, when used together with a robust statistical analysis, are capable of determining conductance and electrical characterization to the single-molecule level. The most popular techniques use either the MCBJ or scanning probes. Conceptually, the MCBJ is a straightforward technique; it relies on forming a pair of proximal electrode contacts, whose separation can be controlled by bending an underlying flexible support. This pair of electrodes can be formed by cleaving a very fine or notched wire mounted on a flexible substrate, but other methods such as electromigration can be used to create the nanogap between the electrodes. The notched metallic structure suspended over an underlying gap can be produced by lithographic

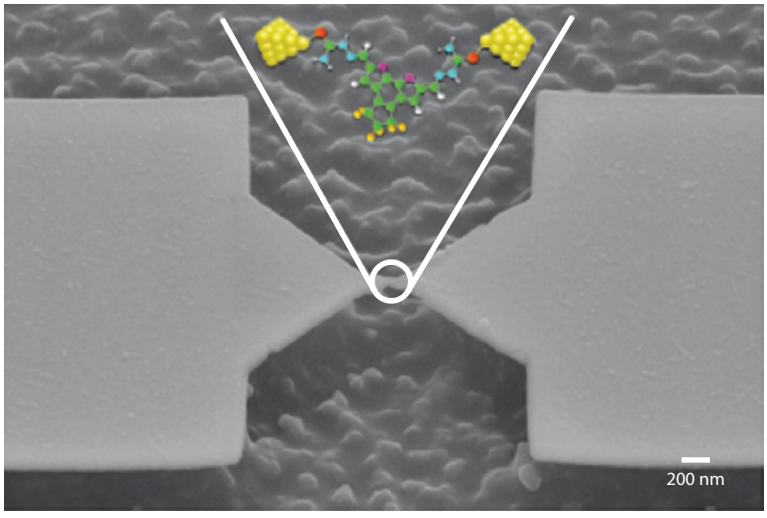

Figure 1

A scanning electron microscopy image of a mechanically controlled break junction with an illustration of a single-molecule trapped in the cleaved gap. From Reference 22, used by permission of the corresponding author E. Scheer.

fabrication. **Figure 1** shows an electron micrograph of a suspended MCBJ with gold electrodes. The bridge is stretched until only a single Au-Au atom bridge connects between the two metal strips. For clean gold, this single-atom bridge has a conductance of G_0 (sometimes referred to as a conductance quantum) with a value of ~77 μS. Upon further stretching, this metallic contact breaks, and the metal contacts snap back to open a gap of typically ~0.6 nm for gold. Molecules can adsorb into this nanogap, and the gap spacing can be increased until the molecular junction itself snaps. The metal contacts can be repeatedly pushed together and opened, to create and then break single gold atom contacts followed by molecular junctions over and over again; this enables many junctions to be measured and, as described below, statistically analyzed.

The MCBJ technique was originally devised for the measurement of the electrical properties of atomic-scale metallic constructions (11), but in 1997 Reed et al. (12) showed that it could be used to study current flow through metal-molecule-metal bridges. These original studies lacked a robust statistical analysis of the molecular junction breaking traces, which was later implemented by Xu & Tao (13) with the in situ scanning tunneling microscope (STM) break junction technique. Nevertheless, these seminal MCBJ experiments by Reed et al. (12), and those in the following few years, demonstrated the possibility of electrical measurements on very few (possibly, single) molecules in metallic nanogaps (14, 15). These studies have now been followed by MCBJ studies of molecular junctions with statistical datasets used to determine single-molecule conductance (16–18); this statistical analysis is similar to the conductance histogram representation used earlier for the analysis of the conductance of atomic-scale metallic constrictions (19–21).

An alternative technique for forming single-molecule junctions, devised by Cui and Lindsay in 2001, employs nanoparticles for forming top contacts to molecules combined with a conducting atomic force microscope (c-AFM) and statistical analysis over many junctions (23). The target molecules, for example octanedithiol (ODT), are adsorbed into self-assembled monolayers (SAMs) on the gold substrate together with octanethiol (OT); the ODT is at high dilution with respect to

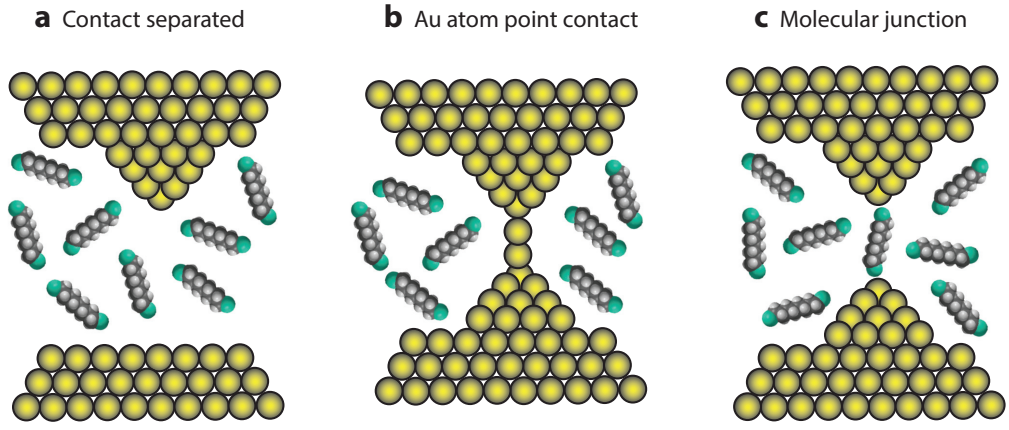

Figure 2

An illustration of the in situ scanning tunneling microscope (STM) break junction technique as innovated by Xu & Tao (13). The STM tip in a solution containing the analyte molecules (*a*) is driven toward the surface and then retracted until a single atomic point contact between the metal surface and STM tip is formed (*b*). Upon further retraction, the metallic junction snaps and molecules can bridge the resulting gap (*c*). If the STM is further retracted, then the molecular junction itself is broken, returning the situation to that of panel *a*. This process can be repeated to form and break many metal atom point contacts followed by molecular junctions. These many junction-making and -breaking events can be then statistically analyzed with conductance histograms to get the metallic atomic point conductance and also the single-molecule junction conductance. The molecular target alternatively can be preadsorbed on the metal substrate.

the OT matrix. Gold nanoparticles (GNPs) are then selectively bound to thiol end groups of ODT to form metal-molecule-metal junctions. Electrical measurements, for instance current-voltage curves (from which junction conductance is determined), are recorded by bringing the c-AFM tip into contact with the top of a GNP (23). With the high dilutions of ODT in OT, single-molecule junctions prevail, and these can be distinguished through many repeated electrical measurements over many nanoparticle junctions. If very small GNPs are used, then quantum charging of the GNP has to be taken into account (24). Nevertheless, it has been shown that for alkanedithiol model systems, this method gives conductance values comparable to other methods such as the in situ break junction and $I(s)$ and $I(t)$ methods described below (24, 25).

The in situ break junction method is conceptually similar to MCBJ technique (13). The in situ break junction technique, however, uses an STM to repeatedly form and cleave metal-to-metal contacts between the STM tip and the substrate surface (see **Figure 2**). The STM tip, which is initially displaced above the metallic (typically gold) substrate, is then driven into it. As the STM tip is withdrawn, the metallic contact thins down, eventually forming a single-atom-wide constriction (**Figure 2*b***). As the tip is further retracted, this snaps and molecular bridges form in the resulting gap (**Figure 2*c***), similar to the process described above for MCBJs. As for MCBJs, this process of junction formation and cleavage can be repeated to form large statistical datasets for junction conductance, as well as other properties such as Seeback coefficients or junction breaking force. Current-voltage curves can also be recorded by pausing the retraction with the molecule bridge in place. A more recent development of the STM break junction technique is the STM jump-to-contact method developed by the Mao group (26–28). In this method, a foreign metal is electrodeposited on the STM tip, and then as the tip approaches the surface under electrochemical potential control metal can be transferred to the substrate. This versatile technique is particularly appropriate for creating metal-molecule-metal junctions from metals other than gold, such as Cu, Ag, and Pd (26–28).

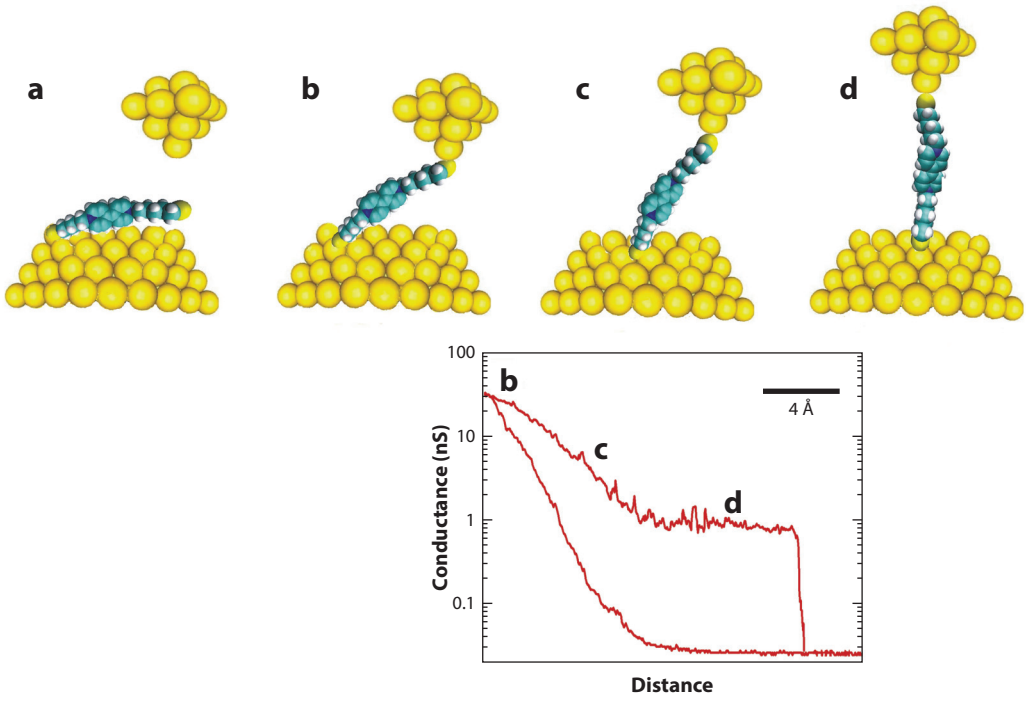

Figure 3

(*a–c*) A schematic illustration of the formation of a molecular bridge from a viologen molecular target with thiol anchor groups at the end of the molecule. From *a* to *c*, the scanning tunneling microscope tip is used to form the molecular junction and extend it in the junction, with cleavage of the molecular bridge following further extension from *d*. Metallic contact between the tip and surface is avoided in this *I*(*s*) technique. The upper line of the plot shows junction conductance at various illustrated stages of the extension of the molecular bridge. A plateau, synonymous with molecular bridge formation, occurs and the conductance suddenly drops as the molecular bridge is broken after *d*. For comparison, the lower curve shows the exponential decay of junction conductance in the absence of molecular bridge formation. Reproduced from Reference 4 with permission from the PCCP Owner Societies.

The *I*(*s*) or *I*(*z*) technique (*I* for current, and *s* or *z* for tip retraction distance, respectively), introduced by Haiss et al. (29) in 2003, is related to the in situ break junction technique in that an STM is used to form molecular junctions and in a similar manner the electrical properties of these junctions are statistically analyzed by repeatedly forming and breaking the junctions. However, the *I*(*s*) technique differs from the in situ break junction technique in that no metallic break junction is formed; instead, the STM tip is approached very close to the sample surface and molecular bridges between the STM and surface stochastically form (29). In this way, the *I*(*s*) and the related *I*(*t*) method described below can be considered noncontact modes of forming single-molecule junctions; these techniques have also been referred to as fishing-mode. **Figure 3** illustrates the *I*(*s*) technique, with the STM tip approaching the surface but avoiding contact, then a molecular junction being formed and then stretched in the junction until it breaks. The noncontact methods can be advantageous in circumstances where tip crashing of the in situ break junction method is best avoided, for instance for measurements with semiconductors or carbon electrodes. This technique has also been used for the formation of junctions by hydrogen bonding of dissimilar SAMs on the molecular functionalized STM tip and substrate surface (30). Hence, by

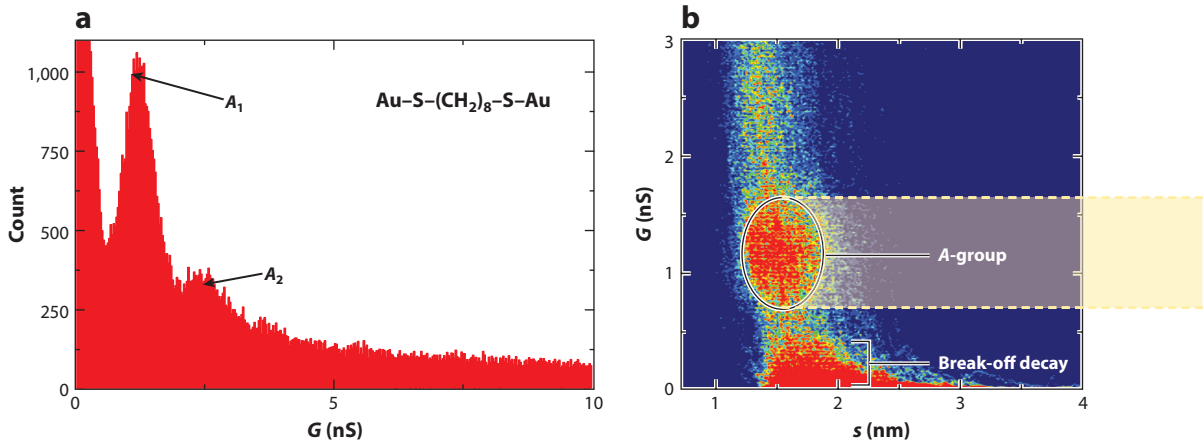

Figure 4

(*a*) A conductance histogram recorded by the *I*(*s*) method for octanedithiol with gold contacts in an ionic liquid medium. The *A*- or low conductance group region is shown. (*b*) A 2D histogram including distance information and showing the low (*A*-) conductance group marked with the ellipsoid encircling the high count (*red*) region. A high count region is also seen for molecular junction breaking at the base of the histogram. Adapted with permission from Reference 31. Copyright 2011, American Chemical Society.

employing the *I*(*s*) method and avoiding direct contact between tip and substrate the asymmetric junction conditions with different molecules on the tip and substrate could be maintained.

It is not enough to record single current-distance curves such as shown in **Figure 3** for the analysis of single-molecule properties when using the in situ break junction, MCBJ, or *I*(*s*) techniques. On the contrary, many hundreds or thousands of such curves have to be recorded and statistically analyzed to reliably obtain single-molecule electrical data averaged over many junction-making and -breaking events. These are collected together in either current or conductance histograms (**Figure 4*a***), or 2D histograms that retain distance information (**Figure 4*b***). An example of such for ODT formed with gold contacts measured with the *I*(*s*) technique in an ionic liquid medium is shown in **Figure 4*a*** (31). The low conductance region is shown with the *A*- or low conductance group marked as A_1 (see Section 3 for a discussion on multiple conductance groups). A small peak, marked A_2, is also seen at double this conductance, which is attributed to two molecules in the junction. These conductance features are relatively sharp and clearly defined, which is often the case for thiol anchoring groups. In other cases, very broad conductance histograms can be seen with the absence of multiple molecule peaks; this is particularly the case for break junction data with certain anchoring groups. These broad histogram features may be the result of averaging over many junctions and contact configurations to give the broad peak, which may also envelop both single and multiple molecules in the junctions and possibly also events where the molecular target is only properly covalently bound to one contact. The *I*(*s*) technique, which avoids tip crashing, is likely to result in measurements on a smoother substrate and this notion is borne out by the observation of lower conductance and sharper histogram peaks assigned to surface coordination on flatter contacts (25).

Data can be analyzed by taking all current-distance traces for anchoring group types where there is a large "hit rate" for junction formation. As an alternative to using unselected current-distance traces, a rational selection criterion can be applied, with the aim of selecting traces where there is clear evidence for stable molecular junction formation. Stable molecular junctions give

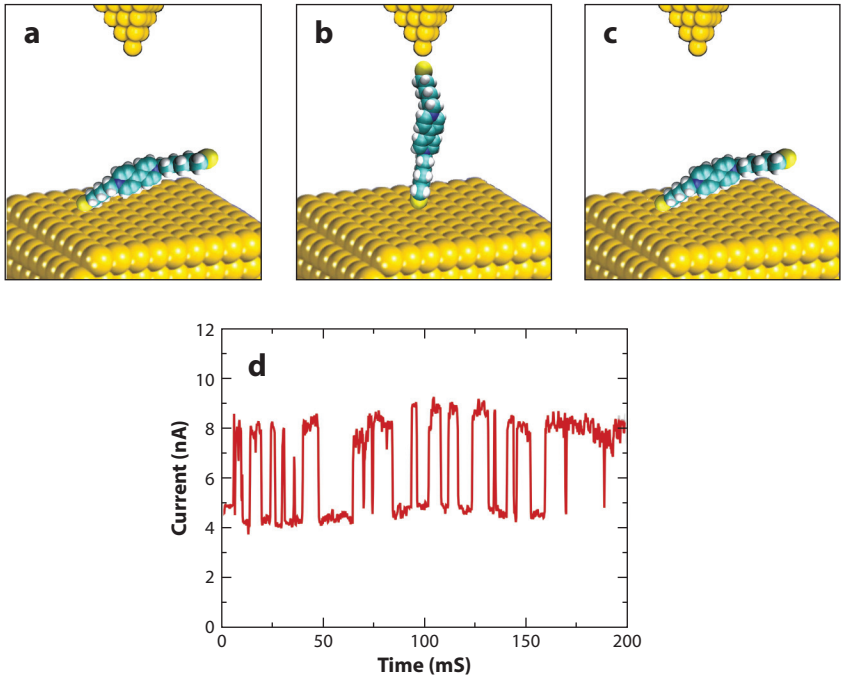

Figure 5

(*a–c*) A schematic illustration of the current-time [*I*(*t*) (37)] method of forming molecular bridges in the gap between a substrate surface and a scanning tunneling microscope tip maintained at a constant height with the feedback loop disabled. (*d*) The plot shows the "blinking" of the current as molecular junctions stochastically form and break. Reproduced from Reference 4 with permission from the PCCP Owner Societies.

extended current plateaus in the retraction curves such as shown in **Figure 3**, and this can be used as a criterion for selection; for example, only curves giving rise to plateaus greater in length than 0.3 nm could be selected. Such a criterion is helpful in cases where there is a relatively low probability for junction formation. This can be the case with the noncontact *I*(*s*) technique, or where surface anchor groups have a tendency to stochastically hop between surface bonding sites if the junction-making process is unstable, leading to a significant number of "noisy" traces (this may occur for thiol contacts) (32, 33). This "noise" may be related to the on-off stochastic switching in wired molecules with thiol contacts (within SAMs), as Ramachandran et al. (34) discuss. The analogous histogram analysis to that described above for current-distance curves can also be applied to current voltage (*I-V*) traces recorded during the junction formation period.

Another STM-based method for single-molecule electrical measurements is the so-called *I*(*t*) technique (current = *I*, time = *t*). If the STM tip is sufficiently close to the surface then current jumps, or "blinks," may be observed in the current-versus-time profiles as molecules stochastically bridge between the tip and surface, forming junctions. **Figure 5** shows a regular pattern of *I*(*t*) jumps over time with the low current level corresponding to tunneling between tip and surface in the absence of bridging molecules and the high current value corresponding to current flow through a bridge. Haiss et al. (25) have analyzed conductance values of model alkanedithiol systems using the in situ break junction, *I*(*s*), Cui-Lindsay nanoparticle junction, and *I*(*t*) methods to show that they all give consistent molecular conductance values (25).

Because the $I(t)$ technique monitors the stochastic formation and cleavage of molecular bridges with time, it can be used to evaluate the relative stability of different types of junctions. Lindsay and coworkers (35) have put this to good use by studying interactions between complementary molecules, with one attached to the STM tip and the other to the substrate surface. When these molecules interact and pair across the junction, for instance by hydrogen bonding, an $I(t)$ current jump is observed, with the average duration of jumps generally related to the junction stability. The formation and stability of junctions of hydrogen-bonded Watson-Crick base pairs, for example, can be studied using this method, and the height and duration of $I(t)$ current blinks can be statistically analyzed; for a range of base pairing interactions, see Section 8 (35).

A further development of the $I(t)$ technique combines the monitoring of the direct current (DC) current jumps resulting from molecular bridge formation with a low amplitude distance modulation of the STM tip (36). This low amplitude mechanical modulation of the tip-surface distance with a frequency of typically ~1 kHz results in an AC signal, which is related to dI/dz (z = distance). This AC signal is sensitive to formation of molecular bridges; when a bridge forms, the AC signal drops sharply, as it is sensitive to the electronic and electromechanical properties of the junction. This combination of simultaneous detection of AC and DC jumps provides an unequivocal signal of molecular bridge formation (36). Because the lifetime of such "on" states can extend for several seconds, during this formation period multiple *I-V* scans or sweeps of the electrochemical potential can be run (7).

Other technique developments include the combination of STM-based molecular conductance measurements with the measurement of other junction parameters, including junction breaking force, thermopower, and transition voltage. Junction stretching and breaking force are measured through a combination of the standard in situ break junction technique and a conducting AFM (38). The junction conductance is conventionally measured and statistically analyzed with the conducting AFM substituting the STM. Force is simultaneously measured during the junction elongation to cleavage and statistically analyzed in force histograms. This method was developed by Xu et al. (38); **Figure 6** provides histogram data from their original publication. **Figure 6*a*,*b*** shows that ODT (C8) single-molecule junctions have a conductance of approximately $2.5 \times 10^{-4}\ G_0$ with a breakdown force of approximately 1.5 nN (38). This breakdown force is similar to that needed to rupture Au-Au bonds, indicating that these may be responsible for breakdown of the thiol connected junctions. However, **Figure 6*c*,*d*** shows bipyridine junctions with conductance of $\sim 10^{-2}\ G_0$ and a breakdown force of ~0.8 nN. The latter is substantially less than the force required to break Au-Au bonds.

Thermopower (or Seeback coefficient) is another highly informative parameter in molecular electronics and single-molecule junction studies. Within a phase coherent tunneling framework (the Landauer formula) the thermopower is given by (39)

$$S_{junction} = -\frac{\pi^2 k_B^2 T}{3\,|e|} \frac{\partial \ln(T(E))}{\partial E}_{E=E_F}, \qquad 1.$$

where S is the Seeback coefficient of the junction, T is the average temperature of the leads, and $T(E)$ is the transmission function of the junction. The transmission function is usually plotted as logarithm of conductance over the considered energy window (E–E_F) and in the simplest case of a single highest occupied molecular orbital (HOMO) and a single lowest unoccupied molecular orbital (LUMO) level representing the electronic structure of the molecular bridge, it displays a plateau region of low conductance, which represents the HOMO-LUMO gap rising with a positive slope at sufficiently positive energy and on the other side (sufficient negative energies) rising with negative slopes. From this and Equation 1, it is immediately apparent that a positive slope and negative $S_{junction}$ corresponds to the Fermi level being aligned closer to the

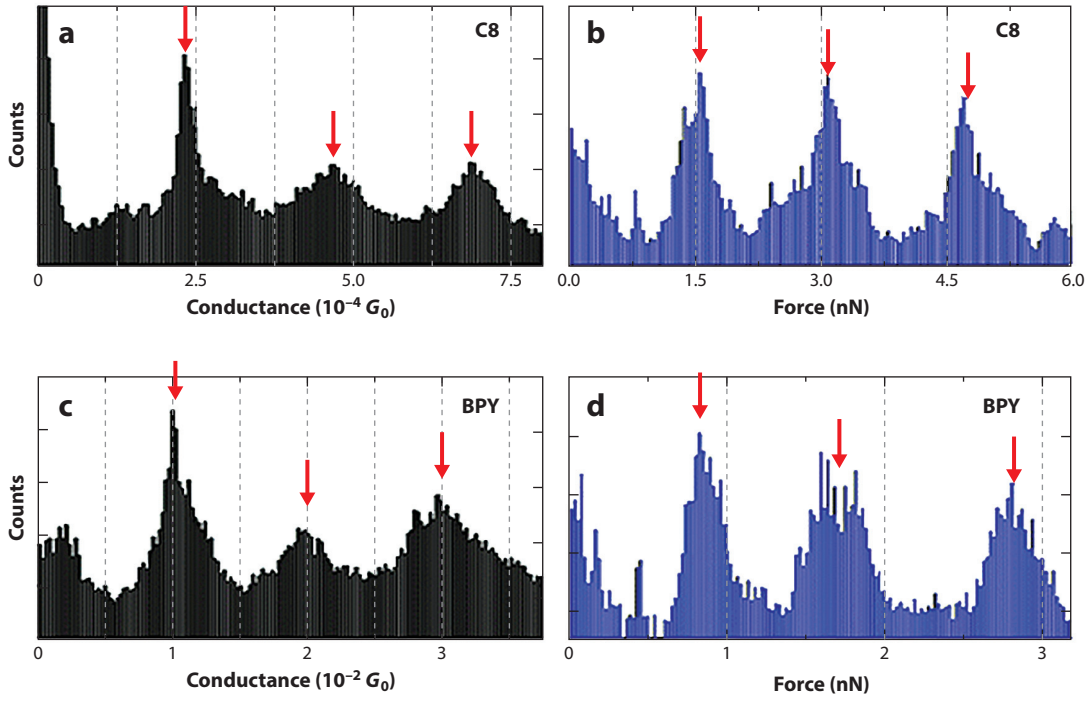

Figure 6

Conductance (*a*,*c*) and force (*b*,*d*) histograms for octanedithiol (C8) (*a*,*b*) and bipyridine (BPY) (*c*,*d*) with gold contacts. Reprinted with permission from Reference 38. Copyright 2003, American Chemical Society.

LUMO, whereas a negative slope and positive $S_{junction}$ corresponds to alignment closer to the HOMO. Using these principles, several groups have shown the strengths of the thermopower technique in determining energy level alignment in molecular junctions and in particular the role of anchoring groups (40–45). **Figure 7** provides a schematic illustration of the STM method for determining the thermoelectric properties of single-molecule junctions. In the STM setup a thermal gradient between the two contacts can be generated with a Peltier element heating (or cooling) the substrate, while the STM tip and the connecting leads are maintained at room temperature. The thermoelectric voltage of the molecular junction can be measured by forming molecular junctions, and then while the molecular junction is in place very briefly setting the externally applied bias voltage to zero (41, 44); alternatively, a low bias voltage *I-V* sweep can be applied with the junction in place (45, 46). In the latter case, the current and voltage offset of the *I-V* curve give the thermoelectric current and voltage of the junction, respectively; the slope of the *I-V* curve gives the junction conductance. For example, the Seeback coefficient of 1,4-benzenedithiol (BDT) with gold contacts, has been determined to be approximately +9 μV/K, with the positive sign indicating closer alignment of E_F to the HOMO level (41). Furthermore, the transmission function of the Au-BDT-Au junction was theoretically derived, and it was deduced from the measured Seeback coefficient that E_F was ~1.2 eV from the HOMO level (41). These concepts have been further developed for a range of functionalized BDT derivatives with methyl-, chloro-, and fluoro- and substituents on the phenyl ring, as well as nitrile anchoring groups replacing

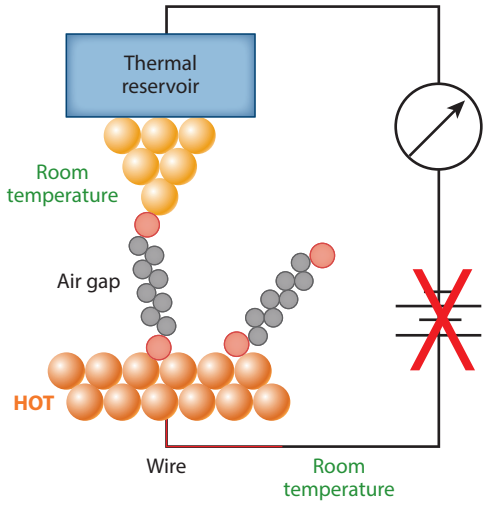

Figure 7

A schematic representation of the measurement of thermopower of a molecular junction with a temperature difference enforced between the substrate and tip. The crossed-out battery sign (*red*) signifies that the thermovoltage can be determined with zero external bias applied. Reprinted with permission from Reference 46. Copyright 2013, American Chemical Society.

the thiol ones (40). The latter case (1,4-benzenedinitrile) showed that the junction conductance switches to being dominated by LUMO transport (40).

3. ANCHORING GROUPS AND CONTACTS

Single-molecule electrical measurements share the commonality that the target molecule must be captured between the two metallic (or semiconducting) electrodes for the electrical measurements to be undertaken. So, in the break junction techniques, for example, molecules attach into the gap as the metallic break junction is created to form a metal-molecule-metal junction. The role of terminal groups at each end of the molecule in anchoring the molecule into the junction is clear. However, their influence on the properties of the molecular junction goes far beyond that, given as described below they can impact junction stability, formation probability, conductance, and current-voltage profiles including current rectification. "Good" anchoring groups are typically seen as those that support relatively high conductance for a given molecular bridge, simultaneously promoting electrically and mechanically stable junctions. In break junction experiments where the nanoscale metallic gap is repeatedly opened and closed, the propensity to form junctions (the hit rate) is also a consideration. Additional considerations have also become apparent, such as the desire to have a lower spread of conductance values, which is apparent in both the width of the conductance histogram distribution and the occurrence of multiple peaks in conductance histograms due to different binding sites of the anchoring group to the electrode. Contact groups may also have more subtle effects, by, for instance, influencing the propensity of molecules to associate or interact with each other in the nanoscale electrical gap. Of course another major consideration is the chemical stability of the terminal group under the environmental and junction formation conditions, although "unstable" terminal groups (leaving groups) have been put to good use in forming direct metal-to-carbon bonding in break junctions, as described below.

At the most basic level, the conductance (G) of a molecular junction can be described by the Landauer formula:

$$G = \frac{2e^2}{h} T_R T_{mol} T_L. \quad 2.$$

The molecular junction is split, somewhat subjectively, into three regions that correspond to transmission at the right and left contacts (T_R and T_L, respectively) and through the backbone of the molecular bridge (T_{mol}). The anchoring groups and the resulting molecule-electrode contacts clearly will have a large bearing on T_R and T_L; given the electronic coupling between anchoring groups and the molecular backbone, they also impact T_{mol}. A single-level resonant tunneling model develops the notion at a simple level of how coupling (or rather scattering) at the contacts and alignment between this single-molecular energy level and the Fermi level of the contacts can control the conductance of the junction. The energy of this molecular level, which could be either a HOMO or LUMO state of the molecule, is ε_0. In this model, the transmission of the junction $T(E,V)$ as a function of energy (E) and bias voltage (V) is given by the Breit-Wigner formula:

$$T(E, V) = \frac{4\Gamma_L \Gamma_R}{(E - \varepsilon_0(V))^2 + (\Gamma_L + \Gamma_R)^2}, \quad 3.$$

where Γ_L and Γ_R are the scattering at the left and right leads. This equation shows plainly how scattering rates, which are related to the strength of the electronic coupling between the molecule and the leads, and level alignment, the $E - \varepsilon_0(V)$ term, control the junction transmission.

The most widely studied electrode material in molecular electronics is gold given its stability, the fact that the surface is oxide free under ambient conditions, and its good electrical conductivity and compatibility with a broad range of chemical anchoring groups. Thiols were the anchoring groups used in the earliest single-molecule studies (12, 13, 23, 29, 37, 47), a fact almost certainly related to the well-established use of thiols for forming SAMs (48, 49). The alkanedithiol system has been viewed as the prototypical model system for studies of single-molecule conductance, in a classical phase coherent tunneling regime with the relatively high (~2 eV) separation between the gold Fermi level and its HOMO frontier orbital of the molecular backbone. Despite the seeming simplicity of this single sulfur atom anchoring to the gold surface, the conductance of alkanedithiols [HS–(CH_2)x–SH] shows several complexities. The early single-molecule studies of alkanedithiols featured a single fundamental conductance value for each molecule type. It later became apparent that multiple conductance "groups" exist, which we discuss in Section 4.

Molecules anchored through nitrogen terminal atoms to gold atoms in particular have also found much popularity in single-molecule electronics. For example, the founding publication of the in situ break junction method by Xu & Tao (13) in 2003 involved the study of 4,4′-bipyridine as well as hexane-, octane-, and decanedithiol. In this study, the measured conductance of 4,4′-bipyridine, at 0.01 G_0, was found to be approximately an order of magnitude higher than hexanedithiol, although later papers attribute a lower conductance to 4,4′-bipyridine (50). Direct nitrogen-to-gold contacting has continued to be one of the most popular anchoring strategies for single-molecule junctions. It has been argued (51) that the conductance of amine-terminated molecules in Au junctions is less variable from junction to junction as a result of the "isotropy of the N lone pair to Au electrode coupling" (p. 461). It is furthermore suggested that amines bind with specificity to under coordinated gold atoms in the junction. Other studies seem to contradict this finding with clear high and low conductance values being observed for alkanes terminated with amines (52). In the latter study, three anchoring groups were compared, namely carboxylic acid (–COOH), amine (–NH_2), and thiol (–SH), with the molecular conductance for a given alkane chain length following the trend thiol > amine > carboxylic acid (52). It was also found that for the amine group– and carboxylic acid group–terminated alkanes, the conductance values are

sensitive to pH due to protonation (–NH_2) or deprotonation (–COOH) of the terminal groups. In a more recent publication, both low and high conductance groups were also observed for tolane with terminal amine groups at each end of the molecule [4,4′-(ethyne-1,2-diyl)dianiline] (53). In this publication it has also been pointed out that aromatic amines have low ionization potentials and rather weak N-H bonds and that they can undergo oxidation reactions and H-atom transfer reactions rather easily, thereby adding a cautionary note to their general deployment (53). Thiols attached to aromatic backbones can also be unstable in the presence of O_2 (53). Furthermore, this study analyzed four different anchoring groups [SH, pyridyl (Py), NH_2, and CN] finding the following trend for junction stability and probability of formation: Py > SH > NH_2 > CN. Pyridyl stood out as an anchoring group in terms of offering relatively high conductance, high formation probability, and chemical robustness. The high junction formation probabilities of –Py and –SH were attributed to a variety of binding geometries and higher binding energy (53).

Alkanes terminated with amines have also been compared with dimethyl phosphine (–PMe_2) and methyl sulfide (–SMe) anchoring groups (54). Junctions could be formed in all three cases with –PMe_2 terminal groups giving the highest conductance, strongest binding energies, and sharpest conductance histograms of this series of molecules (54). Other chemical anchoring groups investigated in single-molecule electronics or multiple molecular junctions include nitrile (–C≡N) (53, 55, 56), isonitrile (–N≡C) (55), thiocyanate (–SCN) (57), isothiocyanate (–NCS) (58–60), nitro (–NO_2) (61), and dithiocarboxylic acid [–C(S)SH] (62). The latter linker is an interesting alternative to thiols, as for conjugated molecules it has been shown to increase conductance (62) and it also boosts the conductance switching in electrochemically switchable single-molecule junctions (63). The majority of systematic single-molecule studies with different anchoring groups have involved gold electrodes, although other anchoring group/electrode combinations have been analyzed, such as, for example, –NC with Pt and –SH and –NCS, with Pt and Pd (59), and amine-terminated oligophenyl and alkane molecular junctions formed with Ag (64).

The anchoring groups discussed above can be generally termed conventional chemically adsorbed contacting groups, or chemicontacts to use the phrase coined in Reference 65. Other larger footprint or multiple attachment point chemicontacts have been investigated, including fullerene contacts (66, 67) and tripodal (68) anchoring groups. The fullerene terminated molecular wires are particularly interesting given they can be imaged with an STM before making single-molecule measurements, thereby guaranteeing that only one molecule is wired into the junction (66, 67). Measurements of dumbbell molecular wires consisting of two C_{60} terminal groups connected through a fluorene and cyclopropyl linker have shown that individual molecules can be repeatedly lifted and pressed back onto the surface, although the highest conductance state was inferred to involve contact between the STM tip and central fluorene group (66). Interestingly, it was also found that the lower conductance state could only be theoretically rationalized by trapping a layer of solvent between Au contact and the fullerene anchoring group (66). Such issues may also need to be considered for certain other anchoring groups in future studies.

Although the above example of the C_{60} anchoring group features direct metal-to-carbon anchoring, linking of single-carbon atoms of the molecular wire backbone to the metal holds great appeal in molecular electronics. Venkataraman and coworkers (69, 70) have achieved such direct gold-to-single-carbon sigma bond linkages. Trimethyltin terminated molecular targets were employed in these studies, namely Me_3Sn–$(CH_2)_x$–$SnMe_3$ and Me_3Sn–CH_2–(phenyl)$_y$–CH_2–$SnMe_3$, with $x = 4$, 6, 10, and 12 and $y = 1$–4, alongside other molecular bridges including Me_3Sn-(phenyl)-$SnMe_3$. These compounds were directly added to the solvent used in the in situ break junction experiments, and it was found that the gold contact atoms displace the trimethyltin-leaving group to form direct Au-C linkages at both ends of the molecular bridges (69, 70). The conductance for the alkanes was found to be ~100 times larger than equivalent alkane bridges

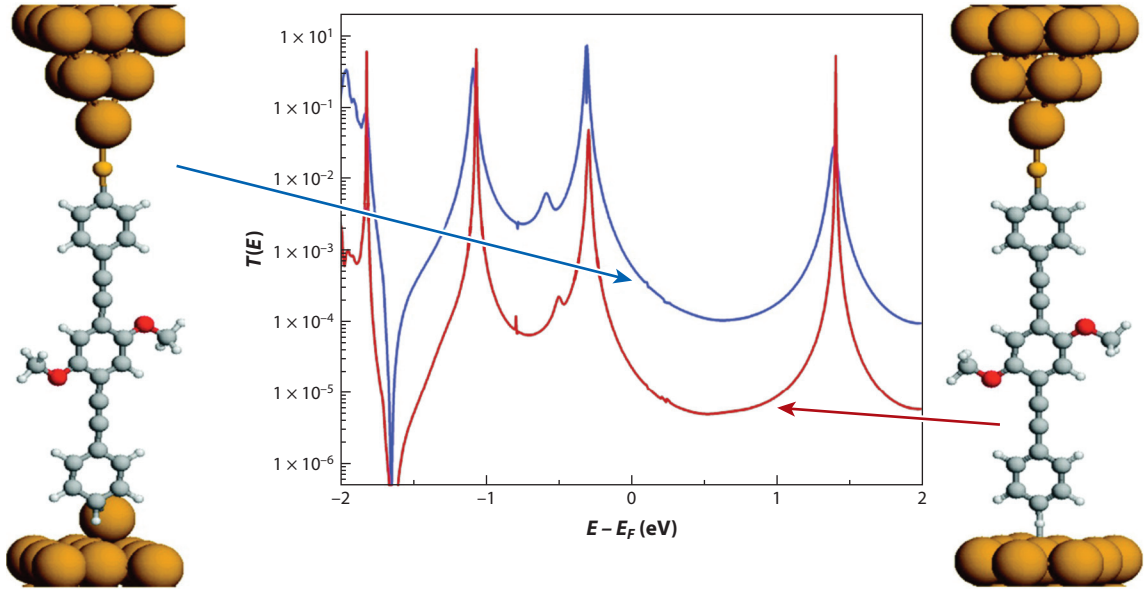

Figure 8

Density functional theory transport computations for a proposed junction configuration for an oligo(phenylene ethynylene) molecular wire terminated at one end by thiol and a plain phenyl group at the other (bottom contact). The phenyl group is shown coordinating with the bottom contact face-on through the end phenyl group to a gold adatom (*blue* transmission curve at *left*) or end-on to a flat gold surface (*red* transmission curve at *right*). The face-on configuration produces a much higher transmission at $E - E_F$. Reprinted with permission from Reference 72. Copyright 2010, American Chemical Society.

terminated with conventional anchoring groups such as amine. A very high conductance of 0.9 G_0 was obtained for Au–CH_2–(phenyl)–CH_2–Au single-molecule junctions (69). A similar approach was used with trimethylsilyl (TMS) terminal groups, where chemical deprotection was used to remove in situ the TMS and aid formation of the Au-C bonds between the metal contacts and molecule bridges in the junction (71).

Contrary to the very strong and highly transmissive Au-C linkages described above, junctions can be formed with much weaker interactions, which are more in line with physisorption rather than covalent bonding or chemisorption. For example, it has been shown using the *I*(*s*) method that single-molecule contacts can be formed to terminal phenyl rings of oligo(phenylene ethynylene) (OPE) molecular wires, where contact is promoted by the interaction between the π-electrons of a terminal phenyl ring and the metal surface (72). **Figure 8** shows theoretical computations justifying such contact configurations for an OPE molecule that is terminated with a conventional thiol chemicontact at one end and a plain phenyl group at the other end (72). Similarly, junctions can be formed with a terminal acetylene (alkyne, –C≡C–H) group (73, 74). It has also been shown to be possible to form junctions with terminal trimethylsilylethynyl (TMSE, –C≡C–$SiMe_3$) and gold electrodes (75–77). Trimethylsilylethynyl had been previously shown to be a contacting group for forming stable SAMs on Au (110, 78–81). In the case of molecular electrical junctions, TMSE was promoted as an anchoring group for simplifying the conductance histograms, given a single low conductance peak was seen rather than the multiple or broad conductance features observed for other anchoring groups such as thiols and pyridyl end groups. It was suggested that this was the result of particular binding configurations of the TMSE group with undercoordinated or step edge atoms (76, 77).

4. MOLECULE-SURFACE COUPLING

In early STM break junction studies, a single conductance value was associated with a given single-molecule junction, for instance Au-bipyridine-Au or Au-ODT-Au. It was later realized that for certain anchoring groups, for instance alkanedithiols and bipyridine, there is no single unique conductance value, but rather several distinct "conductance groups" can exist. Later, it was discovered that conductance could depend on the placement of the molecule with respect to the contacts and that conductance changed as molecules were tilted in the junction or slid along the contacts. These dependencies of junction conductance on the molecule-surface coupling are discussed in this section.

Tao and coworkers (82) identified low conductance and high conductance values for a series of alkanedithiols, which they attributed to the effects of molecule-contact geometries. They suggested that these could correspond to the sulfur end atoms binding at either top or hollow sites of the gold surface. Later, other groups identified three distinct conductance groups [low, medium, and high]. Through examination of the junction breaking distance and also differences between measurements on flat and rough surfaces, as well as through comparison between four different experimental methods to measure single-molecule conductance, Haiss et al. (25) proposed structural models for the different conductance groups based on surface coordination differences. They found that the lowest conductance group occurred with greatest propensity for noncontact, $I(s)$, STM measurements on flat surfaces, whereas rough junctions, such as those created in the break junction method, favored high groups (25). From this observation and the noted junction breaking distances, they concluded that the low groups correspond to sulfur terminal groups attached to single surface atoms, whereas for high groups it was suggested that the sulfur adsorbs to multiple Au atoms at defect or step sites (25). Li et al. (32) have also suggested differences in the microscopic details of contact formation which included differences in binding sites, but for the low conductance group the formation of gauche defects in the alkanethiol chain was also proposed. It is fair to say the complexity of the differing conductance signatures of alkanedithiols has not been fully resolved, with another group reporting the observation of 4 distinct groups (83). In this latter case, different contact resistance values were determined for each group, which was attributed to different electrode-molecule contact configurations (83). Another interesting feature of the alkanedithiol system that has been explored is the influence of the STM-tip gold sample separation on the measured junction conductance. If this is much smaller than the molecular length then the junction will be populated by a large distribution of molecular conformers (84). Because these different conformers generally have different conductance values, the measured conductance is an average over all the accessible conformers. Given the partitioning between conformers depends on temperature, the conductance then becomes temperature dependent for the narrow junctions, whereas it is temperature independent for molecules fully stretched in the junctions into their all-trans alkane chain configuration (84, 85).

The placement of the molecule with respect to the contacts can also have a large impact on the junction conductance. Haiss et al. (86) showed that the conductance of a thiol contacted OPE molecular wire underwent large changes as the spacing between a gold surface and STM tip was changed. Conductance was monitored by the $I(t)$ technique. These conductance changes upon decreasing the spacing between the metal contacts was interpreted on the basis of the conjugated molecular wire tilting in the gap, thereby increasing the coupling to the metal contacts and the transmission of the molecular wire. The plot in **Figure 9** shows the conductance of the rigid molecular wire studied as a function of the gap spacing, with an equivalent molecular tilt angle on the upper x-axis. Upon tilting the molecule from approximately 20° from the vertical orientation to 55°, the conductance increases by more than an order of magnitude (86). The impact of tilting

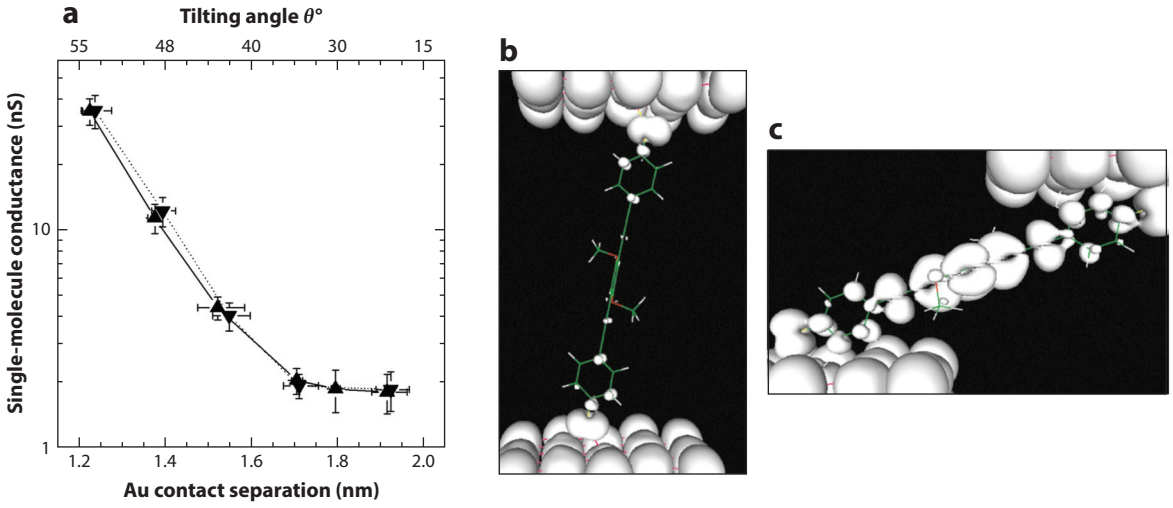

Figure 9

(*a*) The experimentally determined conductance of a long–axially rigid molecular wire OPE1 (1,4-bis[4-(acetylsulphanyl) phenylethynyl]-2,6-dimethoxybenzene) studied as a function of the gap spacing, with an equivalent molecular tilt angle on the upper *x*-axis. Upon tilting the molecule from approximately 20° from the vertical to 55°, the conductance increases by more than an order of magnitude. DFT computed surfaces of constant density of states for OPE1. Two different tilt angles shown are (*b*) y = 10; (*c*) y = 70°. The tilting leads to greatly increased electronic junction conductance. Abbreviations: DFT, density functional theory; OPE, oligo(phenylene ethynylene). Figure reprinted with permission from Reference 86. Copyright 2006, Nature Publishing Group.

on the electronic coupling between molecule and metal contacts is clearly visualized in **Figure 9** with the constant density of states plots computed by density functional theory (DFT). Later, Diez-Perez et al. (87) also analyzed the conductance of a thiol contacted conjugated molecular wire by controlling the angle between the molecule and the two contacts. A novel horizontal mechanical perturbation method was used to modulate the tilt angle and thereby tune the interaction of the molecule with the contacts. The angle of the molecule with the contacts could be changed from a highly tilted state to an orientation nearly perpendicular to the surface, leading to conductance changes of an order of magnitude over this range of tilt angles. In the case of 4,4′-bipyridine, Quek et al. (50) have demonstrated that the conductance of Au-bipyridine-Au junctions can be reversibly switched between high and low conductance states by repeatedly elongating and stretching the junction. The low conductance state is related to a weaker molecule-substrate coupling when the nitrogen-gold bond is perpendicular to the π-system. The high conductance state is achieved in the more compressed junctions by tilting of the molecule, which results in stronger electronic coupling between the molecule and Au contact (50). These respective studies give insight into how different contact geometries, surface coordination, and tilting of the molecule in the gap can impact the junction conductance. Clearly these static snapshots, as they are referred, of the conductance of selected junction configurations represent a simplification of the complexities of the dynamics of the molecular junction evolution as it is first formed and stretched to the breaking point in the break junction experiment. However, promising advances have been made recently in theoretically computing the dynamic evolution of conductance during junction elongation (53, 88, 89). These have included a combination of molecular dynamics simulations and transport computations, and it is expected that development of such approaches will continue, giving further insight into the evolution of different types of single-molecule junctions (53, 88).

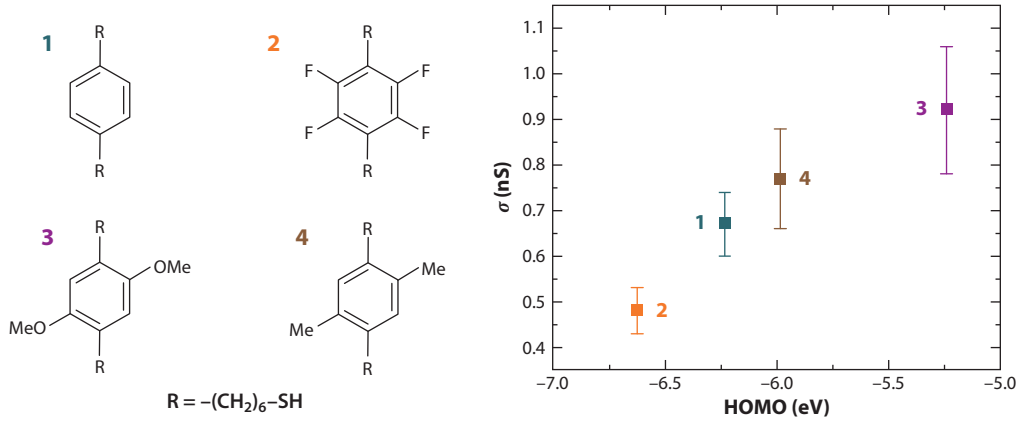

Figure 10

A series of molecular double tunneling barrier molecules with different substituents on the central benzene ring. The molecules were connected to the two gold electrodes with the two R = –$(CH_2)_6$–SH groups. The plot shows single-molecule conductance, determined with the *I*(*t*) method, against the computed HOMO energy of the substituted benzene ring for molecules 1–4. Reproduced with permission from Reference 90. Copyright 2007, The Royal Society of Chemistry.

5. CHEMICAL CONTROL OF JUNCTION CONDUCTANCE

There are many examples of chemical control of single-molecule junction conductance. An early example was from Leary et al. (90) who studied the conductance of a series of 1,4-bis-(6-thiahexyl)-benzene derivatives. This series of molecules consisted of a central benzene ring anchored to the respective gold contacts via two –$(CH_2)_6$–SH groups. These two groups served as tunneling barriers to the central phenyl ring and provided a degree of electronic decoupling between the aromatic ring and the gold contacts. This was envisaged as a molecular double tunneling barrier junction (90). **Figure 10** plots the single-molecule conductance data for four homologues in this series against the computed HOMO energy of the central substituted benzene ring. It can be seen that the more electron-rich benzene rings, with the HOMO levels closer to the gold Fermi energy, give higher conductance. These data are consistent with hole conduction (i.e., via the benzene HOMO); additionally, the high conductance of this whole series compared with HS–$(CH_2)_{12}$–SH, which is the analogous molecule without the central ring, shows that the benzene rings serve as an effective indentation in the tunneling barrier (90).

Another early example of the effect of chemical substituents on single-molecule junction conductance is a series of substituted diaminobenzenes (91). Several substituted molecules were studied with single-molecule conductance ranging from 5.5×10^{-3} G_0 for tetrafluoro-1,4-diaminobenzene to 8.5×10^{-3} G_0 for tetramethyl-1,4-diaminobenzene. It was concluded that charge transport proceeded through the HOMO state, which was closest to the gold Fermi level for electron-donating substituents, consequently showing the highest conductance (91). Xiao et al. (92) have taken another approach to studying chemical substituent effects. Rather than synthesizing the complete series of molecules, they started with one analogue, a nitrosubstituted OPE derivate (OPE–NO_2) with the nitro group on a central benzene ring in the OPE molecular wire, which was attached to the gold electrodes in the junction through thiol groups. They used an electrochemical in situ break junction method to successively reduce the molecule and analyze the conductance. They found that the molecular conductance decreased in the following order according to the OPE ring substituent: $NH_2 > H > NO > NO_2 > NH_3^+$. The latter substituent

was obtained by protonation of OPE–NH_2. The ordering in this series corresponds to the conductance decreasing as the substituent becomes more electron withdrawing, and this was linked with the Hammett substitution parameter (σ), where a larger σ corresponds to a more electron withdrawing substituent (92).

The influence on single-molecule conductance of conjugation between adjacent aromatic rings in molecular bridges has also been studied. With the in situ break junction method, Venkataraman et al. (93) have analyzed the conductance of seven biphenyl molecules that were linked to gold electrodes through amine terminal groups. This series of molecules had different twist angles resulting from different ring substitutions, and they found that the measured junction conductance scaled with the cosine squared of the twist angle between two adjacent phenyl rings. Mishchenko et al. (33) reached a similar conclusion for a series of biphenyl-dithiol derivatives and was supported by accompanying DFT. Sedghi et al. (94) evaluated the conductance versus length of three different families of porphyrin-based wires. They showed that planar edge-fused tapes and alkyne-linked oligomers mediate efficient charge transport far more effectively than twisted singly linked chains. The shallow distance dependence of the conductance of the planar edge-fused tapes and alkyne-linked oligomers was accounted for by the good conjugation and electronic coupling between the porphyrin rings in these oligomers (94). Kolivoska et al. (95) have reported exceptionally low conductance attenuation for a series of extended viologen molecules ($\beta = 0.06\ nm^{-1}$), making these very interesting fully conjugated molecular wires for charge transport to distances in excess of 10 nm.

6. SUPRAMOLECULAR INTERACTIONS IN MOLECULAR JUNCTIONS

Exploiting supramolecular interactions is attractive for the construction of more complex molecular junction assemblies and devices and also for the understanding of charge transport through weaker, noncovalent bonds. **Figure 11** provides examples of supramolecular interactions used in the assembly of molecular junctions with STM break junctions. MCBJ and *I*(*s*) experiments have shown that monothiolated OPE molecular wires can form π-stacking pairs in molecular junctions as long as the molecules are sufficiently long to facilitate strong enough aromatic stacking energetics (**Figure 11*a***) (72, 96). The second example is the formation of junctions through noncovalent

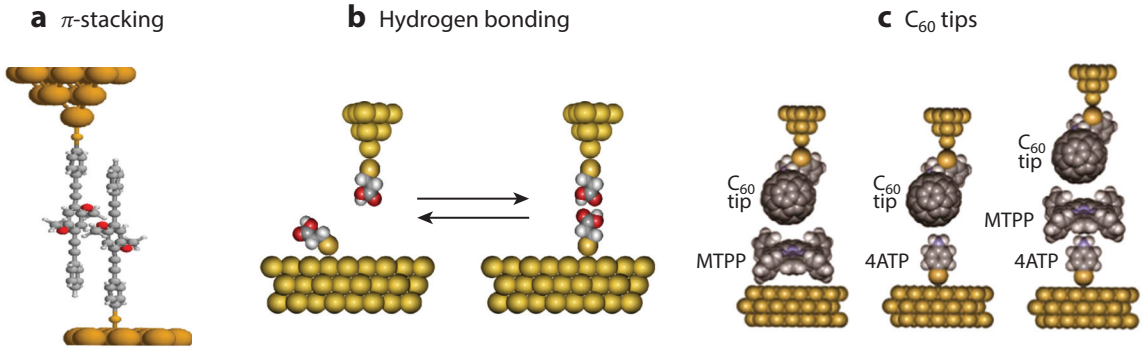

Figure 11

Schematic representations of (*a*) π-stacking, (*b*) hydrogen bonding, and (*c*) supramolecular assembly using fullerene (C_{60}) functionalized STM tips to form a noncovalently linked porphyrin–fullerene dyad. Panel *a* reprinted with permission from Reference 72, panel *b*, from Reference 97, and panel *c*, from Reference 98. Copyright 2010, 2013, and 2013, respectively, American Chemical Society. Abbreviations: ATP, aminothiophenol; MTPP, metallated porphyrin; STM, scanning tunneling microscope.

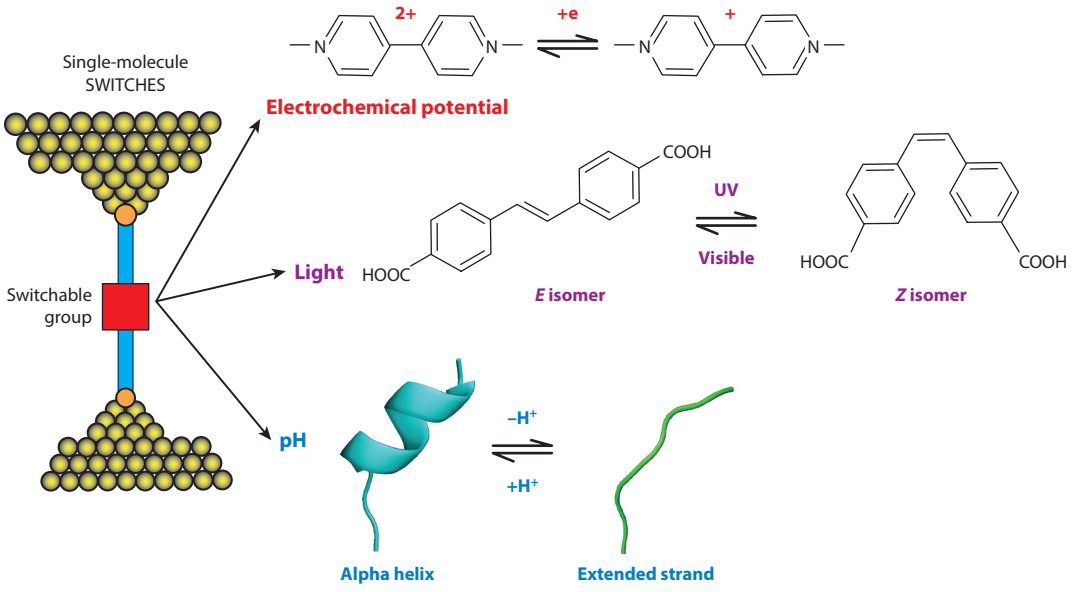

Figure 12

A schematic representation of a range of strategies for switching or gating single-molecule conductance. Lower pH-switching schematic adapted with permission from Reference 103. Copyright 2011, American Chemical Society.

hydrogen bonds between pairs of facing carboxylic acids (**Figure 11*b***) (97). The third example shows the use of a fullerene molecular tip to facilitate assembly of a single noncovalently linked porphyrin–fullerene dyad (**Figure 11*c***) (98).

7. SWITCHING OR GATING SINGLE-MOLECULE CONDUCTANCE

Switching or gating represents one of the most exciting areas of single-molecule electronics with a great deal of different chemical and physical strategies, several of which are illustrated in **Figure 12**. The illustration on the left shows a molecule that contains a switchable group in the electrical junction. A perturbation to the system (e.g., electrochemical potential, illumination, or pH) switches the molecule from one state to another; for example, the top illustration shows electrochemical switching of a viologen moiety from V^{2+} to V^{+} upon making the electrochemical potential sufficiently negative (29, 99). Electrochemical gating is discussed further in the next paragraph. The middle example shows light actuated switching of 4,4′-(ethene-1,2-diyl)dibenzoic acid from its *E* to *Z* isomer (100). The *Z* isomer has been shown through in situ break junctions and *I*(*s*) measurements to exhibit a higher conductance given it facilitates stronger coupling between the phenyl groups and the gold contacts (100). Greater single-molecule conductance switching could be achieved with a photoswitchable dimethyldihydropyrene derivative, through a reversible ring opening/closing isomerization (101). Both of these previous examples represent sequential single-molecule conductance measurements, first of one isomer, followed by photoswitching and then a set of measurements on the other isomer. Battacharyya et al. (102) have taken a very different approach to optical modulation of molecular conductance and have reported large conductance changes through optical excitation of molecular electronic states in an STM break junction setup. Porphyrin–fullerene dyad molecular targets were adsorbed on optically transparent indium tin

oxide (ITO) substrates and these were photoexcited while the conductance was simultaneously monitored using a gold STM tip. The large conductance changes were attributed to long-lived electronically excited states being created, and it was suggested that these resulted from photoexcited charge-separated states being stabilized by the ITO surface (102). The lower example in **Figure 12** shows pH-induced changes in the secondary structure of an oligopeptide molecular bridge, from an alpha helix to an extended strand with increasing pH; we discuss further examples of pH-induced switching of molecular conductance in the following section (103). For more examples of this fascinating topic of molecular switches, see van der Molen & Liljeroth's (9) review.

Electrochemical methods provide a particularly powerful way of controlling the redox state of molecular targets and gating the conductance of single molecules, such as for the viologen example given above. We only briefly discuss this area of research here; recent reviews by Nichols & Higgins (104) and Guo et al. (7) provide more detailed discussions. The electrochemical gating of single molecules has been referred to as a single-molecule transistor configuration using analogies with field effect transistors. Electrochemical gating can be applied in the *I*(*s*) (29), the in situ break junction (13), and MCBJ (105, 106) methods. The addition of a counter and reference electrode to the electrolyte solution and a bipotentiostat helps to control the electrochemical potential of both of the gold contacts independently. The potential is then gated by the electrical double layer that builds up at the metal-solution interfaces. Gating can be highly efficient, with up to 100% of the applied gating potential being experienced by the molecule in the junction. This scenario is very difficult to achieve in solid-state lithographically fabricated three-terminal (gated) nanogaps. Gating in ionic liquids, which are in essence very concentrated liquid electrolytes, can be particularly effective (31, 107). Electrochemical gating allows precise and reproducible control of very strong gating fields in the molecular junction and switching of molecular wires between different chemical redox states. Examples of electrochemical gating of wired single-molecule bridges with the following redox centers include viologens (29, 108–110), pyrrolo-tetrathiafulvalene (pTTF) (107, 111), catechol-type dithiol-terminated OPEs (112), perylene tetracarboxylic bisimides (113–116), oligoanilines (117, 118), anthraquinone (119, 120), and benzodifuran (63). **Figure 13** provides an example of the electrochemical gating of a pTTF molecular bridge. As the electrochemical potential is moved from negative to more positive potentials, the single-molecule conductance increases to give a first peak corresponding to the pTTF/$pTTF^{+}$ redox transition, then falls, and then at more positive electrochemical potentials rises again at the $pTTF^{+}$/$pTTF^{2+}$ redox transition.

8. SENSING AND OUTLOOK

The development of techniques for trapping a single molecule between two electrodes and determining the electrical properties of the resulting junction has obvious potential application in sensing and analysis, potentially down to the single-molecule level. A molecule suitable for this application requires two terminal contact groups for junction formation and a binding site to enable a (preferably reversible) interaction with a target species, such that the interaction modulates the conductance of the junction. Chemically, the most straightforward target for sensing is the proton. That arylamines can serve as contact groups for metal-molecule-metal junction formation (93) has paved way for the possibility of using some well-known pH-sensitive indicator dyes (**Figure 14**) as single-molecule proton sensors, and Li et al. (121) have explored this possibility both theoretically and experimentally. p-Rosaniline is red in weakly acidic conditions, with a conjugated structure and a small HOMO-LUMO separation, but in basic media the central carbon changes from sp^2 to sp^3 hybridization upon OH^{-} attack, removing the conjugation and hence decolorizing the molecule by greatly increasing its HOMO-LUMO separation (calculated as 2.78 eV for the red form and 5.03 eV for the colorless form). The arylamine groups were found

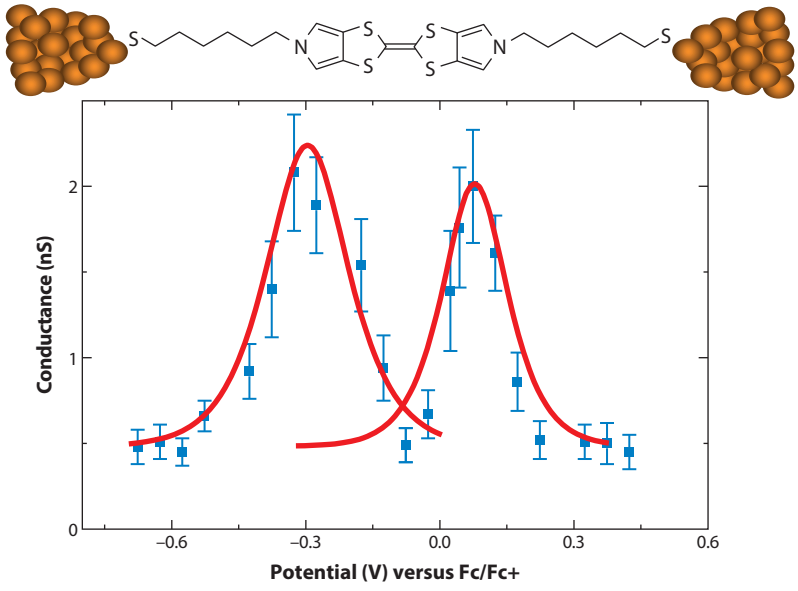

Figure 13

Electrochemical gating of 6pTTF6 in an ionic liquid electrolyte with gold electrodes. The change of single-molecule conductance measured with the *I*(*s*) technique is shown as a function of the electrochemical potential. Reprinted with permission from Reference 107. Copyright 2012, American Chemical Society.

to act as contacts in STM break junction experiments. At pH 5.5, the conductance was 72 ± 9 nS, whereas at pH 13.6 it decreased to 0.73 ± 0.10 nS, a factor of 100 times smaller. Because small molecules like this conduct by tunneling, a lower conductance for the nonconjugated form with its much larger HOMO-LUMO separation is expected, given the contact Fermi energy falls within the HOMO-LUMO gap and the conductance is a function of the separation between the Fermi energy and the energy of the frontier orbital (HOMO or LUMO) involved in transport. Interestingly, although α,ω–bis(dimethylamino) alkanes were earlier shown not to form junctions with gold contacts (51), Malachite green (MG) (**Figure 14**) did give measurable conductances in STM break junction experiments (121), perhaps because the adjacent aryl groups assist in junction formation; the conductance of junctions involving MG fell from 66 ± 13 nS in acid to 0.72 ± 0.10 nS in base.

Xiao et al. (122) in 2004 performed one of the first demonstrations of chemical sensing using a single-molecule junction. They used short peptides (cysteamine-Cys, cysteamine-Gly-Cys, Cys-Gly-Cys, and cysteamine-Gly-Gly-Cys; see **Figure 15** for the latter), with two terminal thiol groups provided by cysteine and/or cysteamine units for making contact with gold electrodes (**Figure 15**). They investigated the effect of metal ion complexation on the junction conductances of these peptides. The conductances generally increased upon metal ion (Ni^{2+}, Cu^{2+}) complexation, with by far the largest increases observed for the longer peptides, in which there are more binding sites for the metal ions. Metal ion binding by adsorbed peptides on gold was established by cyclic voltammetry given (at least in the case of the longer peptides) the metal complexes have a reversible one-electron redox wave [assigned in the paper as Cu(II)/Cu(I), but more likely to be Cu(II)/Cu(III); see Reference 123]. The metal ions are known to bind to the longer peptides in square planar geometry via deprotonated amide nitrogens (with the terminal peptide—NH_2 in this case; see also **Figure 15**). The largest effect, a 320-fold increase in conductance, was found for

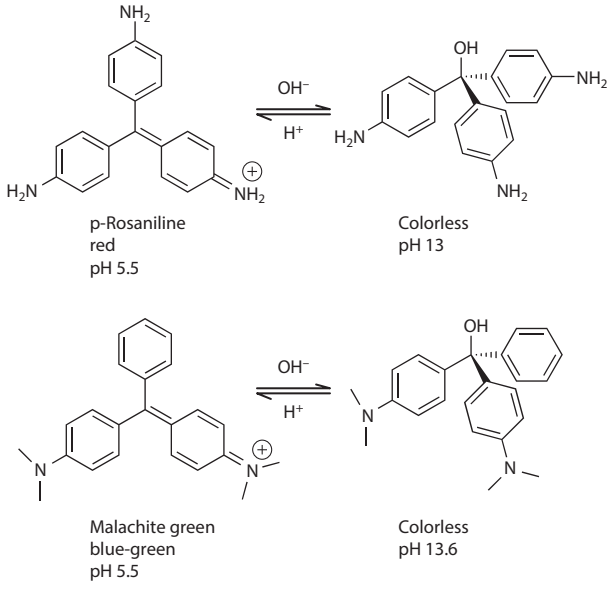

Figure 14

Well-known pH-sensitive indicator dyes explored as single-molecule proton sensors.

cysteamine-Gly-Gly-Cys upon binding Cu^{2+}. Two factors may contribute to this very sizeable conductance increase. One is the major change in peptide conformation, and hence a shorter gold-gold distance in the junction, upon formation of the square planar complex, as indicated in **Figure 15**. The other is the possibility of new conduction paths through the molecule as a consequence of the presence of covalent metal-ligand bonds in the complex (122).

There are examples in nature of long-range electron transfer processes mediated via hydrogen bonds, sometimes involving water molecules occupying special positions within the supramolecular structure (124). Consequently, there has been much interest in, for example, photophysical studies of biomimetic donor-acceptor systems in which the reacting species are connected by hydrogen bonds (125) and electrochemical studies in which a redox species H-bonds to a SAM on an electrode surface (126). Not surprisingly, therefore, it was not long after the development of techniques for studying metal-molecule-metal junctions that attempts were made to fabricate metal-molecule. . .molecule-metal junctions, in which the two molecules are each anchored to one electrode via a strong covalent bond, typically a thiol, and are connected to each other by H-bonds. Chang et al. (127) provided an early example in which thiol-functionalized nucleotides were

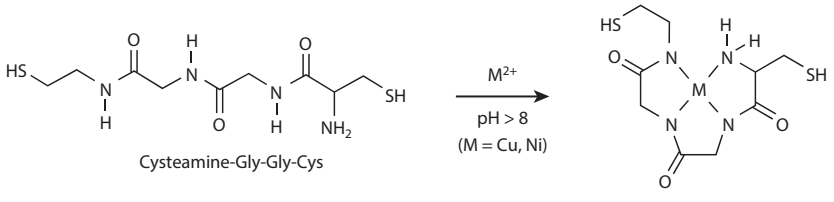

Figure 15

Cysteamine-Gly-Gly-Cys used in sensing metal ion (Ni^{2+}, Cu^{2+}) complexation.

attached to gold STM tips and gold substrates. A steady tunnel current set-point was established under servo-control, the servo was broken, and the current-distance decay curve was then recorded on tip retraction. It was found that junctions held together by three hydrogen bonds (guanine–deoxycytidine and 2-aminoadenine-thymidine) gave current-distance signals that extended further than those held together by two (adenine-thymidine or 2-aminoadenine-deoxycytidine), and control experiments established that very rapid decay was observed if the tip was covered in a non-H-bonding thiol. Conducting AFM (c-AFM) was used to measure the stiffness of the H-bonds, and the force-distance curves for approach and retraction processes. The overall conclusion was that conductances of all of the H-bonded junctions were quite similar because of the highly non-transmissive sugar unit in the nucleosides, whereas the mechanical properties of the junctions were distinguishable, for example in current-retraction distance curves (127). This work does not, however, involve specifically single-molecule junctions, given the nucleosides were present on the substrate in a SAM, and the STM and c-AFM tips were estimated to be making initial contact with 2–10 molecules, depending on the set-point current.

Zwolak & Di Ventra (128) suggested the possibility of sequencing DNA by passing a single strand of DNA through a nanoelectrode gap and measuring the tunneling currents through the different bases. This has stimulated the Lindsay group (129) to extend their work on H-bonded molecules in junctions to attempt to distinguish individual DNA bases via H-bonding. In this work, both a gold STM tip and a gold substrate were coated with 4-mercaptobenzamide, which has a potential H-bond donor (the amide $-NH_2$) and an acceptor (the amide C=O) (129). The tip was held a distance from the substrate that resulted in very small tunneling gap conductance (<20 pS) in aqueous buffer, and from tunnel decay experiments it was estimated that the tip-substrate distance was then slightly longer than two mercaptobenzamide molecules. Nucleotides were then introduced into the solution. Telegraphic noise signals were observed in the current-time response. The intensity, duration and repetition rates of these were distinguishable for the four different DNA bases. The interpretation is that these signals occur when a single base molecule temporarily H-bonds to both tip and substrate and provides an unusually short tunneling path. Experiments were also conducted with short DNA oligomers (e.g., CCACC), in which the tip effectively sampled the bases at random, and distinguishable signals characteristic of each base were observed (129). This opens the possibility of using tunneling via H-bonded junctions to sequence DNA, as long as the DNA could be transported sequentially across the tunnel junction site. A similar approach has very recently been described for amino acids (130), although protein sequencing with 22 naturally occurring amino acids would undoubtedly be more challenging than DNA sequencing, with only 4 bases to distinguish.

Given the progress of this work on fabricating tunneling junctions by allowing an H-bonded network spontaneously to form in the gap, and the characterization of supramolecular junctions via π-stacking interactions (see Section 6), it is perhaps surprising that little work has been reported on the effect of other intermolecular interactions on metal-molecule-metal junctions. It was established fairly early that the conductance of junctions involving alkanedithiols was not significantly affected by the medium; experiments in ambient, under aqueous electrolyte, perfluorocarbons, hydrocarbon liquids, or in ultra high vacuum, all resulted in the same conductance values within experimental error (4), and more recently this has been extended to ionic liquids (31). In the case of alkane backbones, the HOMO-LUMO separations are very large (the frontier orbitals are far from the contact Fermi energy), so any small modulation of these energies by changing the environment would not be expected to affect the junction conductance significantly. However, with π-conjugated systems, particularly those with small HOMO-LUMO separations, this is not necessarily the case.

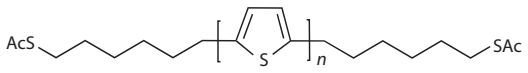

Figure 16

Molecular target containing oligothiophene in the chain.

It was found experimentally that the conductances of single-molecule junctions involving a series of hexanethiol-contacted oligothiophenes (**Figure 16**) did not vary significantly with the length of the molecule, although transport calculations using a DFT/nonequilibrium Greens function approach predicted that the conductances should fall exponentially with length (131). The π-systems of thiophene units interact significantly with water molecules, and transport calculations carried out using water molecules included in their energy-minimized positions showed that the transport resonances of the molecules were shifted significantly by the water interactions. The longer and more conjugated the molecule, the smaller was the HOMO-LUMO gap and so the larger was the predicted effect upon the molecular junction conductance, so that the experimental data was then reproduced quite well by the calculations. In follow-up experiments, the conductances of the molecular junctions were then determined in the absence of water, by using an argon-purged atmosphere chamber and also by carrying out measurements in UHV. After a 24-h argon purge, and using the terthiophene ($n = 3$) molecule, a 100-fold decrease in the molecular conductance in the absence of water was noted, and the conductance of the pentathiophene molecule was too low in the absence of water to be measured (4, 131).

Thiophenes are electron-rich aromatic systems, and donor-acceptor charge transfer interactions have played a major role in the early history of organic electronics, providing the first examples of an organic metal (tetrathiafulvalene.tetracyanoquinodimethane; TTF:TCNQ) and an organic superconductor ($[TMTSF]_2PF_6$; TMTSF = tetramethyl-tetraselenofulvalene) (132). This has now prompted a study of the effects of the strong electron acceptor, tetracyanoethylene (TCNE) upon the electrical properties of junctions involving the terthiophene ($n = 3$; **Figure 16**). The earlier work on the effect of water on the conductances of oligothiophenes had focused on just one conductance value, but in this more recent study, using the STM break junction technique, three conductance values were found for 1,2,4-trichlorobenzene solutions of the terthiophene in **Figure 16** recorded in the presence of excess TCNE, at $165 \times 10^{-6}\ G_0$, $570 \times 10^{-6}\ G_0$, and $1{,}860 \times 10^{-6}\ G_0$ (4). (The observation of three different conductance values is in accord with work on alkanedithiols, where it has been suggested that the three values are seen because the thiol contact atom can take up two different contact geometries, either bound to a flat gold surface or in proximity with a gold step edge.) In the absence of TCNE, three values of the conductance of the terthiophenes were also seen, at $2.5 \times 10^{-6}\ G_0$, $9 \times 10^{-6}\ G_0$, and $41 \times 10^{-6}\ G_0$. These values are, respectively, a factor of 66, 63, and 45 lower. Transport calculations reveal that when terthiophene forms a complex with TCNE, an additional transport resonance results, and this is close to the contact Fermi energy, causing a very significant increase in conductance (A. Vezzoli, I.M. Grace, C. Brooke, C.J. Lambert & R.J. Nichols, unpublished data).

Taken together, these studies all pave way to possible future applications of metal-molecule-metal junctions in chemical and biological sensing, perhaps even down to the single-molecule level, offering potentially exciting avenues for new single-molecule technologies and detection systems in sensing and analytical sciences.

DISCLOSURE STATEMENT

The authors are not aware of any affiliations, memberships, funding, or financial holdings that might be perceived as affecting the objectivity of this review.

LITERATURE CITED

1. Aviram A, Ratner MA. 1974. Molecular rectifiers. *Chem. Phys. Lett.* 29:277–83
2. Metzger RM. 1999. Electrical rectification by a molecule: the advent of unimolecular electronic devices. *Acc. Chem. Res.* 32:950–57
3. Tao NJ. 2006. Electron transport in molecular junctions. *Nat. Nanotechnol.* 1:173–81
4. Nichols RJ, Haiss W, Higgins SJ, Leary E, Martin S, Bethell D. 2010. The experimental determination of the conductance of single molecules. *Phys. Chem. Chem. Phys.* 12:2801–15
5. Aradhya SV, Venkataraman L. 2013. Single-molecule junctions beyond electronic transport. *Nat. Nanotechnol.* 8:399–410
6. Chen F, Hihath J, Huang ZF, Li XL, Tao NJ. 2007. Measurement of single-molecule conductance. *Annu. Rev. Phys. Chem.* 58:535–64
7. Guo S, Manuel Artes J, Diez-Perez I. 2013. Electrochemically-gated single-molecule electrical devices. *Electrochim. Acta* 110:741–53
8. Kiguchi M, Kaneko S. 2013. Single molecule bridging between metal electrodes. *Phys. Chem. Chem. Phys.* 15:2253–67
9. van der Molen SJ, Liljeroth P. 2010. Charge transport through molecular switches. *J. Phys. Condensed Matter* 22:133001
10. Lindsay SM, Ratner MA. 2007. Molecular transport junctions: clearing mists. *Adv. Mater.* 19:23–31
11. Agrait N, Yeyati AL, van Ruitenbeek JM. 2003. Quantum properties of atomic-sized conductors. *Phys. Rep.* 377:81–279
12. Reed MA, Zhou C, Muller CJ, Burgin TP, Tour JM. 1997. Conductance of a molecular junction. *Science* 278:252–54
13. Xu BQ, Tao NJJ. 2003. Measurement of single-molecule resistance by repeated formation of molecular junctions. *Science* 301:1221–23
14. Kergueris C, Bourgoin JP, Palacin S, Esteve D, Urbina C, et al. 1999. Electron transport through a metal-molecule-metal junction. *Phys. Rev. B* 59:12505–13
15. Weber HB, Reichert J, Weigend F, Ochs R, Beckmann D, et al. 2002. Electronic transport through single conjugated molecules. *Chem. Phys.* 281:113–25
16. Gonzalez MT, Wu SM, Huber R, van der Molen SJ, Schonenberger C, Calame M. 2006. Electrical conductance of molecular junctions by a robust statistical analysis. *Nano Lett.* 6:2238–42
17. Huber R, Gonzalez MT, Wu S, Langer M, Grunder S, et al. 2008. Electrical conductance of conjugated oligomers at the single molecule level. *J. Am. Chem. Soc.* 130:1080–84
18. Smit RHM, Noat Y, Untiedt C, Lang ND, van Hemert MC, van Ruitenbeek JM. 2002. Measurement of the conductance of a hydrogen molecule. *Nature* 419:906–9
19. Krans JM, Vanruitenbeek JM, Fisun VV, Yanson IK, Dejongh LJ. 1995. The signature of conductance quantization in metallic point contacts. *Nature* 375:767–69
20. Olesen L, Laegsgaard E, Stensgaard I, Besenbacher F, Schiotz J, et al. 1995. Reply to "Comment on: 'Quantized conductance in an atom-sized point-contact.'" *Phys. Rev. Lett.* 74:2147
21. Gai Z, He Y, Yu HB, Yang WS. 1996. Observation of conductance quantization of ballistic metallic point contacts at room temperature. *Phys. Rev. B* 53:1042–45
22. Briechle BM, Kim Y, Ehrenreich P, Erbe A, Sysoiev D, et al. 2012. Current-voltage characteristics of single-molecule diarylethene junctions measured with adjustable gold electrodes in solution. *Beilstein J. Nanotechnol.* 3:798–808
23. Cui XD, Primak A, Zarate X, Tomfohr J, Sankey OF, et al. 2001. Reproducible measurement of single-molecule conductivity. *Science* 294:571–74
24. Morita T, Lindsay S. 2007. Determination of single molecule conductances of alkanedithiols by conducting-atomic force microscopy with large gold nanoparticles. *J. Am. Chem. Soc.* 129:7262–63

25. Haiss W, Martin S, Leary E, van Zalinge H, Higgins SJ, et al. 2009. Impact of junction formation method and surface roughness on single molecule conductance. *J. Phys. Chem. C* 113:5823–33
26. Zhou X-S, Liang J-H, Chen Z-B, Mao B-W. 2011. An electrochemical jump-to-contact STM-break junction approach to construct single molecular junctions with different metallic electrodes. *Electrochem. Commun.* 13:407–10
27. Peng Z-L, Chen Z-B, Zhou X-Y, Sun Y-Y, Liang J-H, et al. 2012. Single molecule conductance of carboxylic acids contacting Ag and Cu electrodes. *J. Phys. Chem. C* 116:21699–705
28. Wang Y-H, Zhou X-Y, Sun Y-Y, Han D, Zheng J-F, et al. 2014. Conductance measurement of carboxylic acids binding to palladium nanoclusters by electrochemical jump-to-contact STM break junction. *Electrochim. Acta* 123:205–10
29. Haiss W, van Zalinge H, Higgins SJ, Bethell D, Hobenreich H, et al. 2003. Redox state dependence of single molecule conductivity. *J. Am. Chem. Soc.* 125:15294–95
30. Bui PT, Nishino T. 2014. Electron transfer through coordination bond interaction between single molecules: conductance switching by a metal ion. *Phys. Chem. Chem. Phys.* 16:5490–94
31. Kay NJ, Nichols RJ, Higgins SJ, Haiss W, Sedghi G, et al. 2011. Ionic liquids as a medium for STM-based single molecule conductance determination: an exploration employing alkanedithiols. *J. Phys. Chem. C* 115:21402–8
32. Li C, Pobelov I, Wandlowski T, Bagrets A, Arnold A, Evers F. 2008. Charge transport in single Au—alkanedithiol—Au junctions: coordination geometries and conformational degrees of freedom. *J. Am. Chem. Soc.* 130:318–26
33. Mishchenko A, Vonlanthen D, Meded V, Buerkle M, Li C, et al. 2010. Influence of conformation on conductance of biphenyl-dithiol single-molecule contacts. *Nano Lett.* 10:156–63
34. Ramachandran GK, Hopson TJ, Rawlett AM, Nagahara LA, Primak A, Lindsay SM. 2003. A bond-fluctuation mechanism for stochastic switching in wired molecules. *Science* 300:1413–16
35. Chang S, He J, Lin L, Zhang P, Liang F, et al. 2009. Tunnel conductance of Watson-Crick nucleoside-base pairs from telegraph noise. *Nanotechnology* 20:185102
36. Xia JL, Diez-Perez I, Tao NJ. 2008. Electron transport in single molecules measured by a distance-modulation assisted break junction method. *Nano Lett.* 8:1960–64
37. Haiss W, Nichols RJ, van Zalinge H, Higgins SJ, Bethell D, Schiffrin DJ. 2004. Measurement of single molecule conductivity using the spontaneous formation of molecular wires. *Phys. Chem. Chem. Phys.* 6:4330–37
38. Xu BQ, Xiao XY, Tao NJ. 2003. Measurements of single-molecule electromechanical properties. *J. Am. Chem. Soc.* 125:16164–65
39. Paulsson M, Datta S. 2003. Thermoelectric effect in molecular electronics. *Phys. Rev. B* 67:241403
40. Baheti K, Malen JA, Doak P, Reddy P, Jang S-Y, et al. 2008. Probing the chemistry of molecular heterojunctions using thermoelectricity. *Nano Lett.* 8:715–19
41. Reddy P, Jang SY, Segalman RA, Majumdar A. 2007. Thermoelectricity in molecular junctions. *Science* 315:1568–71
42. Malen JA, Doak P, Baheti K, Tilley TD, Segalman RA, Majumdar A. 2009. Identifying the length dependence of orbital alignment and contact coupling in molecular heterojunctions. *Nano Lett.* 9:1164–69
43. Tan A, Balachandran J, Sadat S, Gavini V, Dunietz BD, et al. 2011. Effect of length and contact chemistry on the electronic structure and thermoelectric properties of molecular junctions. *J. Am. Chem. Soc.* 133:8838–41
44. Widawsky JR, Darancet P, Neaton JB, Venkataraman L. 2012. Simultaneous determination of conductance and thermopower of single molecule junctions. *Nano Lett.* 12:354–58
45. Evangeli C, Gillemot K, Leary E, Teresa Gonzalez M, Rubio-Bollinger G, et al. 2013. Engineering the thermopower of C_{60} molecular junctions. *Nano Lett.* 13:2141–45
46. Guo S, Zhou G, Tao N. 2013. Single molecule conductance, thermopower, and transition voltage. *Nano Lett.* 13:4326–32
47. Reichert J, Ochs R, Beckmann D, Weber HB, Mayor M, von Lohneysen H. 2002. Driving current through single organic molecules. *Phys. Rev. Lett.* 88:176804

48. Nuzzo RG, Allara DL. 1983. Adsorption of bifunctional organic disulfides on gold surfaces. *J. Am. Chem. Soc.* 105:4481–83
49. Ulman A. 1996. Formation and structure of self-assembled monolayers. *Chem. Rev.* 96:1533–54
50. Quek SY, Kamenetska M, Steigerwald ML, Choi HJ, Louie SG, et al. 2009. Mechanically controlled binary conductance switching of a single-molecule junction. *Nat. Nanotechnol.* 4:230–34
51. Venkataraman L, Klare JE, Tam IW, Nuckolls C, Hybertsen MS, Steigerwald ML. 2006. Single-molecule circuits with well-defined molecular conductance. *Nano Lett.* 6:458–62
52. Chen F, Li X, Hihath J, Huang Z, Tao N. 2006. Effect of anchoring groups on single-molecule conductance: comparative study of thiol-, amine-, and carboxylic-acid-terminated molecules. *J. Am. Chem. Soc.* 128:15874–81
53. Hong W, Manrique DZ, Moreno-Garcia P, Gulcur M, Mishchenko A, et al. 2012. Single molecular conductance of tolanes: experimental and theoretical study on the junction evolution dependent on the anchoring group. *J. Am. Chem. Soc.* 134:2292–304
54. Park YS, Whalley AC, Kamenetska M, Steigerwald ML, Hybertsen MS, et al. 2007. Contact chemistry and single-molecule conductance: a comparison of phosphines, methyl sulfides, and amines. *J. Am. Chem. Soc.* 129:15768–69
55. Kiguchi M, Miura S, Hara K, Sawamura M, Murakoshi K. 2006. Conductance of a single molecule anchored by an isocyanide substituent to gold electrodes. *Appl. Phys. Lett.* 89:213104
56. Mishchenko A, Zotti LA, Vonlanthen D, Buerkle M, Pauly F, et al. 2011. Single-molecule junctions based on nitrile-terminated biphenyls: a promising new anchoring group. *J. Am. Chem. Soc.* 133:184–87
57. Yamada R, Kumazawa H, Noutoshi T, Tanaka S, Tada H. 2008. Electrical conductance of oligothiophene molecular wires. *Nano Lett.* 8:1237–40
58. Fu MD, Chen WP, Lu HC, Kuo CT, Tseng WH, Chen CH. 2007. Conductance of alkanediisothiocyanates: effect of headgroup-electrode contacts. *J. Phys. Chem. C* 111:11450–55
59. Ko C-H, Huang M-J, Fu M-D, Chen C-H. 2010. Superior contact for single-molecule conductance: electronic coupling of thiolate and isothiocyanate on Pt, Pd, and Au. *J. Am. Chem. Soc.* 132:756–64
60. Yin C, Huang G-C, Kuo C-K, Fu M-D, Lu H-C, et al. 2008. Extended metal-atom chains with an inert second row transition metal: $[Ru_5(\mu_5\text{-tpda})_4X_2]$ ($tpda^{2-}$ = tripyridyldiamido dianion, X = Cl and NCS). *J. Am. Chem. Soc.* 130:10090–92
61. Zotti LA, Kirchner T, Cuevas J-C, Pauly F, Huhn T, et al. 2010. Revealing the role of anchoring groups in the electrical conduction through single-molecule junctions. *Small* 6:1529–35
62. Xing Y, Park T-H, Venkatramani R, Keinan S, Beratan DN, et al. 2010. Optimizing single-molecule conductivity of conjugated organic oligomers with carbodithioate linkers. *J. Am. Chem. Soc.* 132:7946–56
63. Li Z, Li H, Chen S, Froehlich T, Yi C, et al. 2014. Regulating a benzodifuran single molecule redox switch via electrochemical gating and optimization of molecule/electrode coupling. *J. Am. Chem. Soc.* 136:8867–70
64. Kirn T, Vazquez H, Hybertsen MS, Venkataraman L. 2013. Conductance of molecular junctions formed with silver electrodes. *Nano Lett.* 13:3358–64
65. Salomon A, Cahen D, Lindsay S, Tomfohr J, Engelkes VB, Frisbie CD. 2003. Comparison of electronic transport measurements on organic molecules. *Adv. Mater.* 15:1881–90
66. Gillemot K, Evangeli C, Leary E, La Rosa A, Teresa Gonzalez M, et al. 2013. A detailed experimental and theoretical study into the properties of C_{60} dumbbell junctions. *Small* 9:3812–22
67. Leary E, Gonzalez MT, van der Pol C, Bryce MR, Filippone S, et al. 2011. Unambiguous *one*-molecule conductance measurements under ambient conditions. *Nano Lett.* 11:2236–41
68. Ie Y, Hirose T, Nakamura H, Kiguchi M, Takagi N, et al. 2011. Nature of electron transport by pyridine-based tripodal anchors: potential for robust and conductive single-molecule junctions with gold electrodes. *J. Am. Chem. Soc.* 133:3014–22
69. Chen W, Widawsky JR, Vazquez H, Schneebeli ST, Hybertsen MS, et al. 2011. Highly conducting Π-conjugated molecular junctions covalently bonded to gold electrodes. *J. Am. Chem. Soc.* 133:17160–63
70. Cheng ZL, Skouta R, Vazquez H, Widawsky JR, Schneebeli S, et al. 2011. In situ formation of highly conducting covalent Au-C contacts for single-molecule junctions. *Nat. Nanotechnol.* 6:353–57

71. Hong W, Li H, Liu S-X, Fu Y, Li J, et al. 2012. Trimethylsilyl-terminated oligo(phenylene ethynylene)s: an approach to single-molecule junctions with covalent au-c sigma-bonds. *J. Am. Chem. Soc.* 134:19425–31
72. Martin S, Grace I, Bryce MR, Wang C, Jitchati R, et al. 2010. Identifying diversity in nanoscale electrical break junctions. *J. Am. Chem. Soc.* 132:9157–64
73. Osorio HM, Cea P, Ballesteros LM, Gascon I, Marques-Gonzalez S, et al. 2014. Preparation of nascent molecular electronic devices from gold nanoparticles and terminal alkyne functionalised monolayer films. *J. Mater. Chem. C* 2:7348–55
74. Marina Ballesteros L, Martin S, Momblona C, Marques-Gonzalez S, Carmen Lopez M, et al. 2012. Acetylene used as a new linker for molecular junctions in phenylene-ethynylene oligomer Langmuir-Blodgett films. *J. Phys. Chem. C* 116:9142–50
75. Millar D, Venkataraman L, Doerrer LH. 2007. Efficacy of Au-Au contacts for scanning tunneling microscopy molecular conductance measurements. *J. Phys. Chem. C* 111:17635–39
76. Marques-Gonzalez S, Yufit DS, Howard JAK, Martin S, Osorio HM, et al. 2013. Simplifying the conductance profiles of molecular junctions: the use of the trimethylsilylethynyl moiety as a molecule-gold contact. *Dalton Trans.* 42:338–41
77. Pera G, Martin S, Ballesteros LM, Hope AJ, Low PJ, et al. 2010. Metal-molecule-metal junctions in Langmuir-Blodgett films using a new linker: Trimethylsilane. *Chem.-Eur. J.* 16:13398–405
78. Marchenko A, Katsonis N, Fichou D, Aubert C, Malacria M. 2002. Long-range self-assembly of a polyunsaturated linear organosilane at the n-Tetradecane/Au(111) interface studied by STM. *J. Am. Chem. Soc.* 124:9998–99
79. Katsonis N, Marchenko A, Taillemite S, Fichou D, Chouraqui G, et al. 2003. A molecular approach to self-assembly of trimethylsilylacetylene derivatives on gold. *Chemistry* 9:2574–81
80. Katsonis N, Marchenko A, Fichou D, Barrett N. 2008. Investigation on the nature of the chemical link between acetylenic organosilane self-assembled monolayers and Au(111) by means of synchrotron radiation photoelectron spectroscopy and scanning tunneling microscopy. *Surf. Sci.* 602:9–16
81. Watcharinyanon S, Nilsson D, Moons E, Shaporenko A, Zharnikov M, et al. 2008. A spectroscopic study of self-assembled monolayer of porphyrin-functionalized oligo(phenyleneethynylene)s on gold: the influence of the anchor moiety. *Phys. Chem. Chem. Phys.* 10:5264–75
82. Li XL, He J, Hihath J, Xu BQ, Lindsay SM, Tao NJ. 2006. Conductance of single alkanedithiols: conduction mechanism and effect of molecule-electrode contacts. *J. Am. Chem. Soc.* 128:2135–41
83. Zhou J, Chen F, Xu B. 2009. Fabrication and electronic characterization of single molecular junction devices: a comprehensive approach. *J. Am. Chem. Soc.* 131:10439–46
84. Haiss W, van Zalinge H, Bethell D, Ulstrup J, Schiffrin DJ, Nichols RJ. 2006. Thermal gating of the single molecule conductance of alkanedithiols. *Faraday Discuss.* 131:253–64
85. Jones DR, Troisi A. 2007. Single molecule conductance of linear dithioalkanes in the liquid phase: apparently activated transport due to conformational flexibility. *J. Phys. Chem. C* 111:14567–73
86. Haiss W, Wang C, Grace I, Batsanov AS, Schiffrin DJ, et al. 2006. Precision control of single-molecule electrical junctions. *Nat. Mater.* 5:995–1002
87. Diez-Perez I, Hihath J, Hines T, Wang Z-S, Zhou G, et al. 2011. Controlling single-molecule conductance through lateral coupling of pi orbitals. *Nat. Nanotechnol.* 6:226–31
88. Paulsson M, Krag C, Frederiksen T, Brandbyge M. 2009. Conductance of alkanedithiol single-molecule junctions: a molecular dynamics study. *Nano Lett.* 9:117–21
89. Kamenetska M, Koentopp M, Whalley AC, Park YS, Steigerwald ML, et al. 2009. Formation and evolution of single-molecule junctions. *Phys. Rev. Lett.* 102:126803
90. Leary E, Higgins SJ, van Zalinge H, Haiss W, Nichols RJ. 2007. Chemical control of double barrier tunnelling in alpha, omega-dithiaalkane molecular wires. *Chem. Commun.* 38:3939–41
91. Venkataraman L, Park YS, Whalley AC, Nuckolls C, Hybertsen MS, Steigerwald ML. 2007. Electronics and chemistry: varying single-molecule junction conductance using chemical substituents. *Nano Lett.* 7:502–6
92. Xiao XY, Nagahara LA, Rawlett AM, Tao NJ. 2005. Electrochemical gate-controlled conductance of single oligo(phenylene ethynylene)s. *J. Am. Chem. Soc.* 127:9235–40

93. Venkataraman L, Klare JE, Nuckolls C, Hybertsen MS, Steigerwald ML. 2006. Dependence of single-molecule junction conductance on molecular conformation. *Nature* 442:904–7
94. Sedghi G, Esdaile LJ, Anderson HL, Martin S, Bethell D, et al. 2012. Comparison of the conductance of three types of porphyrin-based molecular wires: beta, meso, beta-fused tapes, meso-butadiyne-linked and twisted meso-meso linked oligomers. *Adv. Mater.* 24:653
95. Kolivoska V, Valasek M, Gal M, Sokolova R, Bulickova J, et al. 2013. Single-molecule conductance in a series of extended viologen molecules. *J. Phys. Chem. Lett.* 4:589–95
96. Wu SM, Gonzalez MT, Huber R, Grunder S, Mayor M, et al. 2008. Molecular junctions based on aromatic coupling. *Nat. Nanotechnol.* 3:569–74
97. Nishino T, Hayashi N, Bui PT. 2013. Direct measurement of electron transfer through a hydrogen bond between single molecules. *J. Am. Chem. Soc.* 135:4592–95
98. Bui PT, Nishino T, Yamamoto Y, Shiigi H. 2013. Quantitative exploration of electron transfer in a single noncovalent supramolecular assembly. *J. Am. Chem. Soc.* 135:5238–41
99. Gittins DI, Bethell D, Schiffrin DJ, Nichols RJ. 2000. A nanometre-scale electronic switch consisting of a metal cluster and redox-addressable groups. *Nature* 408:67–69
100. Martin S, Haiss W, Higgins SJ, Nichols RJ. 2010. The impact of E-Z photo-isomerization on single molecular conductance. *Nano Lett.* 10:2019–23
101. Roldan D, Kaliginedi V, Cobo S, Kolivoska V, Bucher C, et al. 2013. Charge transport in photoswitchable dimethyldihydropyrene-type single-molecule junctions. *J. Am. Chem. Soc.* 135:5974–77
102. Battacharyya S, Kibel A, Kodis G, Liddell PA, Gervaldo M, et al. 2011. Optical modulation of molecular conductance. *Nano Lett.* 11:2709–14
103. Scullion L, Doneux T, Bouffier L, Fernig DG, Higgins SJ, et al. 2011. Large conductance changes in peptide single molecule junctions controlled by pH. *J. Phys. Chem. C* 115:8361–68
104. Nichols RJ, Higgins SJ. 2014. Single molecular electrochemistry within an STM. In *Electrocatalysis*, Vol. 14: *Theoretical Foundations and Model Experiments*, ed. RC Alkire, DM Kolb, J Lipkowski. Weinham, Ger.: Wiley-VCH
105. Shu C, Li CZ, He HX, Bogozi A, Bunch JS, Tao NJ. 2000. Fractional conductance quantization in metallic nanoconstrictions under electrochemical potential control. *Phys. Rev. Lett.* 84:5196–99
106. Tian J-H, Yang Y, Zhou X-S, Schoellhorn B, Maisonhaute E, et al. 2010. Electrochemically assisted fabrication of metal atomic wires and molecular junctions by MCBJ and STM-BJ methods. *Chemphyschem* 11:2745–55
107. Kay NJ, Higgins SJ, Jeppesen JO, Leary E, Lycoops J, et al. 2012. Single-molecule electrochemical gating in ionic liquids. *J. Am. Chem. Soc.* 134:16817–26
108. Li Z, Han B, Meszaros G, Pobelov I, Wandlowski T, et al. 2006. Two-dimensional assembly and local redox activity of molecular hybrid structures in an electrochemical environment. *Faraday Discuss.* 131:121–43
109. Haiss W, Albrecht T, van Zalinge H, Higgins SJ, Bethell D, et al. 2007. Single-molecule conductance of redox molecules in electrochemical scanning tunneling microscopy. *J. Phys. Chem. B* 111:6703–12
110. Li ZH, Pobelov I, Han B, Wandlowski T, Blaszczyk A, Mayor M. 2007. Conductance of redox-active single molecular junctions: an electrochemical approach. *Nanotechnology* 18:044018
111. Leary E, Higgins SJ, van Zalinge H, Haiss W, Nichols RJ, et al. 2008. Structure-property relationships in redox-gated single molecule junctions—a comparison of pyrrolo-tetrathiafulvalene and viologen redox groups. *J. Am. Chem. Soc.* 130:12204–5
112. Kolivoska V, Moreno-Garcia P, Kaliginedi V, Hong W, Mayor M, et al. 2013. Electron transport through catechol-functionalized molecular rods. *Electrochim. Acta* 110:709–17
113. Li C, Mishchenko A, Li Z, Pobelov I, Wandlowski T, et al. 2008. Electrochemical gate-controlled electron transport of redox-active single perylene bisimide molecular junctions. *J. Phys.-Condens. Matter* 20:374122
114. Li XL, Xu BQ, Xiao XY, Yang XM, Zang L, Tao NJ. 2006. Controlling charge transport in single molecules using electrochemical gate. *Faraday Discuss.* 131:111–20
115. Li C, Stepanenko V, Lin M-J, Hong W, Wuerthner F, Wandlowski T. 2013. Charge transport through perylene bisimide molecular junctions: an electrochemical approach. *Phys. Status Solidi B* 250:2458–67

116. Li X, Hihath J, Chen F, Masuda T, Zang L, Tao N. 2007. Thermally activated electron transport in single redox molecules. *J. Am. Chem. Soc.* 129:11535–42
117. Chen F, Nuckolls C, Lindsay S. 2006. In situ measurements of oligoaniline conductance: linking electrochemistry and molecular electronics. *Chem. Phys.* 324:236–43
118. He J, Chen F, Lindsay S, Nuckolls C. 2007. Length dependence of charge transport in oligoanilines. *Appl. Phys. Lett.* 90:072112
119. Darwish N, Diez-Perez I, Guo SY, Tao NJ, Gooding JJ, Paddon-Row MN. 2012. Single molecular switches: electrochemical gating of a single anthraquinone-based norbornylogous bridge molecule. *J. Phys. Chem. C* 116:21093–97
120. Darwish N, Diez-Perez I, Da Silva P, Tao NJ, Gooding JJ, Paddon-Row MN. 2012. Observation of electrochemically controlled quantum interference in a single anthraquinone-based norbornylogous bridge molecule. *Angew. Chem. Int. Ed.* 51:3203–6
121. Li Z, Smeu M, Afsari S, Xing Y, Ratner MA, Borguet E. 2014. Single-molecule sensing of environmental pH—an STM break junction and NEGF-DFT approach. *Angew. Chem. Int. Ed.* 53:1098–102
122. Xiao XY, Xu BQ, Tao NJ. 2004. Changes in the conductance of single peptide molecules upon metal-ion binding. *Angew. Chem. Int. Ed.* 43:6148–52
123. Pratesi A, Zanello P, Giorgi G, Messori L, Laschi F, et al. 2007. New copper(II)/cyclic tetrapeptide system that easily oxidizes to copper(III) under atmospheric oxygen. *Inorganic Chem.* 46:10038–40
124. Holzenberg A, Scrutton NS, eds. 2002. *Enzyme-Catalyzed Electron and Radical Transfer*, Vol. 35: *Subcellular Biochemistry*. New York, London: Plenum Press
125. Sanchez L, Sierra M, Martin N, Myles AJ, Dale TJ, et al. 2006. Exceptionally strong electronic communication through hydrogen bonds in porphyrin–C_{60} pairs. *Angew. Chem. Int. Ed.* 45:4637–41
126. Sek S, Maicka E, Bilewicz R. 2005. Efficient electron transfer through hydrogen bonded interface. *Electrochim. Acta* 50:4857–60
127. Chang S, He J, Kibel A, Lee M, Sankey O, et al. 2009. Tunnelling readout of hydrogen-bonding-based recognition. *Nat. Nanotechnol.* 4:297–301
128. Zwolak M, Di Ventra M. 2005. Electronic signature of DNA nucleotides via transverse transport. *Nano Lett.* 5:421–24
129. Huang S, He J, Chang S, Zhang P, Liang F, et al. 2010. Identifying single bases in a DNA oligomer with electron tunnelling. *Nat. Nanotechnol.* 5:868–73
130. Zhao Y, Ashcroft B, Zhang P, Liu H, Sen S, et al. 2014. Single-molecule spectroscopy of amino acids and peptides by recognition tunnelling. *Nat. Nanotechnol.* 9:466–73
131. Leary E, Hobenreich H, Higgins SJ, van Zalinge H, Haiss W, et al. 2009. Single-molecule solvation-shell sensing. *Phys. Rev. Lett.* 102:086801
132. Bryce MR. 1991. Recent progress on conducting organic charge-transfer salts. *Chem. Soc. Rev.* 20:355–90